Radiolarians from the cyclic Messinian diatomites of Falconara (Sicily, Italy)

Giuseppe CORTESE
Department of Earth Sciences, University of Florence
Via La Pira, 4, 50121 Florence (Italy)
Alfred Wegener Institut for Polar and Marine Research
Columbusstrasse, P.O. Box 120161, 27515 Bremerhaven (Germany)
gcortese@awi-bremerhaven.de

Kjell R. BJØRKLUND
Paleontological Museum, University of Oslo
Sars'gate, 1, 0562 Oslo 5 (Norway)
k.r.bjorklund@toyen.uio.no

Cortese G. & Bjørklund K. R. 1999. — Radiolarians from the cyclic Messinian diatomites of Falconara (Sicily, Italy), *in* De Wever P. & Caulet J.-P. (eds), InterRad VIII, Paris/Bierville 8-13 septembre 1997, *Geodiversitas* 21(4) : 593-624 .

ABSTRACT
The diatomitic sediments in Falconara (6.93 to 6.08 Ma) have a total thickness of *c.* 27 m, and the sequence is composed of 41 diatomite/claystone couplets. The deposition of these biosiliceous sediments, seemingly modulated by the astronomical precession cycle (21,000 years period), has been suggested to have taken place in a shallow basin with diatomaceous and claystone sediments being deposited during low and high sea level stands, respectively. Polycystine radiolarians show major changes in the assemblage compositions and the total abundances between the different cycles, from being barren in Cycle 2 till > 142,000 radiolarians/g in Cycle 26. Radiolarians are usually not present in the claystone samples, this is also the case with diatoms. However, one claystone (S11) had a significant high number, > 43,000 radiolarians/g sediment, while nine others had a low content of radiolarians. We have in our counts recognised 68 morphotypes. Q-Mode Factor analysis has been used on the raw counting data. By using five factors, we were able to explain 83.65% of the cumulative variance, while using nine factors allowed us to explain 96.52% of the variance. These nine factors displayed well-defined peaks that can be used to navigate within the profile and to correlate between sections. Another high resolution stratigraphical tool could be represented by the peculiar faunal composition of each of the diatomites. In our pilot study we selected three diatomites and

KEY WORDS
Radiolaria,
Miocene,
Italy,
ciclicity.

compared their assemblage composition and radiolarian abundances. Cycle 11 is dominated by *Stichocorys delmontensis* and *Lithomitra lineata*, *c.* 50 and 36% maximum values respectively. In Cycle 21, *S. delmontensis* and *Botryostrobus auritus/australis* are most common, with 40 and 30% as maximum values respectively. In both these cycles nassellarians are the dominant group. In Cycle 26 Larcoidea sp., *Porodiscus* sp., and *Spongotrochus glacialis* are the dominant taxa.

RÉSUMÉ

Radiolaires des sédiments messiniens à diatomées de Falconara (Sicile, Italie).

Les sédiments à diatomées de Falconara (agés de 6,93 à 6,08 millions d'années) ont une épaisseur totale d'environ 27 m. La séquence est composée de 41 paires diatomite/argile. Le dépôt de ces sédiments biosiliceux est apparemment modulé par le cycle de précession astronomique (avec une période de 21000 ans) et semble avoir eu lieu dans un bassin peu profond; les sédiments à diatomées et argileux correspondent respectivement à des périodes de bas et haut niveau marin. La composition des assemblages à radiolaires polycystines et l'abondance de ceux-ci varient beaucoup d'un cycle à l'autre, d'absent dans le cycle 2 jusqu'à plus de 142000 radiolaires/g dans le cycle 26. Les radiolaires, ainsi que les diatomées, sont généralement absents des échantillons argileux. Cependant, une argile (S11) a une concentration élevée (> 43000 radiolaires/g) et neuf autres ont une faible concentration. Nous avons compté 68 morphotypes. Les données brutes ont été soumises à une analyse factorielle en mode Q. Avec cinq facteurs, nous pouvons expliquer 83,65 % de la variance cumulée, tandis que neuf facteurs sont nécessaires pour rendre compte de 96,52 % de cette variance. Ces neufs facteurs montrent des maximums bien définis qui peuvent être utilisés pour naviguer le long du profil et pour corréler les différentes coupes. Une autre méthode permettant une bonne résolution stratigraphique pourrait être fondée sur la faune particulière à chacune de ces diatomites. Dans une étude pilote, nous avons choisi trois diatomites et nous avons comparé la composition de leurs assemblages et leur abondance en radiolaires. Le cycle 11 est dominé par *Stichocorys delmontensis* et *Lithomitra lineata*, avec des maximum à environ 50 % et 36 % respectivement. Dans le cycle 21, *S. delmontensis* et *Botryostrobus auritus/australis* sont les plus communs, avec des maximum à environ 40 % et 30 % respectivement. Pour ces deux cycles, les nassellaires forment le groupe dominant. Dans le cycle 26, Larcoidea sp., *Porodiscus* sp., et *Spongotrochus glacialis* sont les taxons dominants.

MOTS CLÉS
Radiolaires,
Miocène,
Italie,
périodicité.

INTRODUCTION

The biogenic siliceous sediments of Sicily have been known for almost 125 years. Ehrenberg (1854) and Mottura (1871) reported on radiolarians from the Sicilian Neogene, while Sauvage (1873) described, in fairly good detail, foliated, radiolarian bearing shale outcrops near Licata (Fig. 1). He assigned a Messinian-Zanclean age to them. Stöhr (1876, 1878) and Schwager (1878) studied Tortonian and Zanclean diatomites and tuffs containing rich radiolarian assemblages. Nicotra (1882) examined Tortonian diatomites containing radiolarians near Messina.

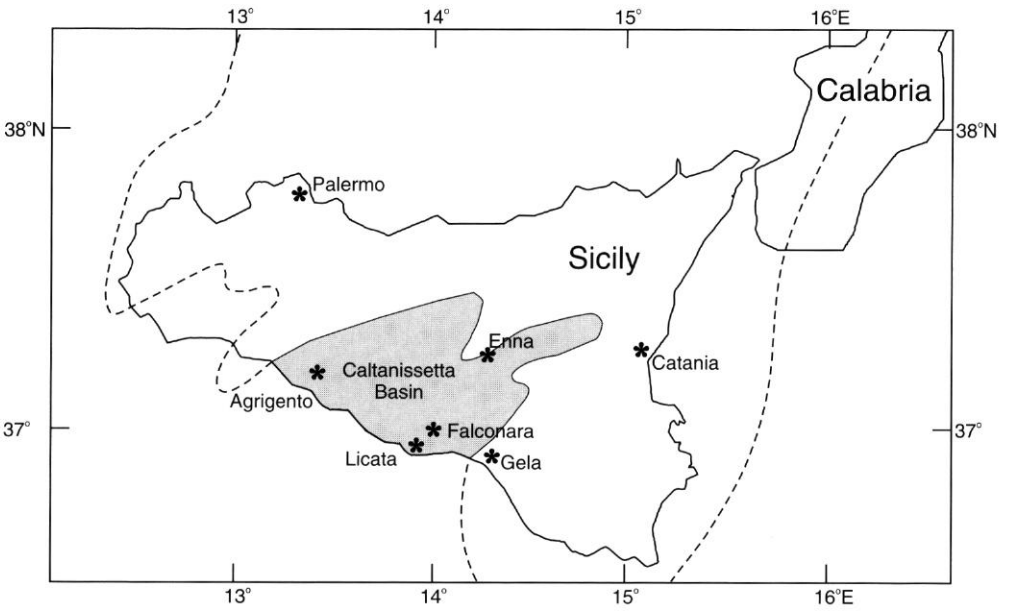

FIG. 1. — Location map, showing the geographical position of the Falconara Section. The shaded area represents the Caltanissetta Basin, while the solid line depicts the paleo-shore line. Modified from Gautier (1994).

Cocco (1905) did the same with different lithologies (marls, tuffs, diatomites) outcropping at several Sicilian localities.

Several cruises of the Deep Sea Drilling Project (DSDP) and of the Ocean Drilling Program (ODP) have taken place in the Mediterranean Sea: DSDP Legs 13, 42, ODP Legs 107, 160 and 161, and biogenic opal bearing localities from the former Tethys Sea area have been reported on by several authors as: Sanfilippo (1971, 1974), Sanfilippo *et al.* (1973), Rio *et al.* (1989). All these authors failed to apply the standard radiolarian biostratigraphic scheme for tropical latitudes, or to establish a local one.

Biogenic opal is generally not well preserved in the Neogene sediments of the Mediterranean Sea (Dumitrica 1973; Riedel *et al.* 1985). The latter authors report on only eight deep-sea localities in the Mediterranean Sea where siliceous remains are present in isolated levels. Moreover, at several of these localities the radiolarians are scarce or present in only a few of the samples. Furthermore, the species that are used in the standard low latitude stratigraphical radiolarian scheme are found in low numbers and are often morphologically different from the true oceanic ones.

Messinian siliceous diatomitic oozes outcrop at many localities in the Caltanissetta Basin, Sicily. These sediments yield abundant and diversified radiolarian faunas, thus having a potential for the compilation of a new local radiolarian stratigraphy based on acme zones and peak occurrences, through calibrations with other microfossil groups. As we could not apply the standard low latitude biostratigraphical radiolarian scheme to the Falconara Section, we used Q-mode factor analysis to facilitate faunal comparisons between samples as an alternative tool for correlation. This allows us to recognise, through time, different associations being indicative of specific ecological settings (i.e. peak occurrences), events that later may be used as a correlation tool both within the Falconara Section and between other sections in the Caltanissetta Basin.

Hilgen & Krijgsman (1999) stress the uncertainty and controversy about both the age of the Tripoli Formation and the origin of the cyclic bedding (Gautier *et al.* 1993; Butler *et al.* 1995; McClelland *et al.* 1996; Sprovieri *et al.* 1996; Vai 1997). They also summarise the following scena-

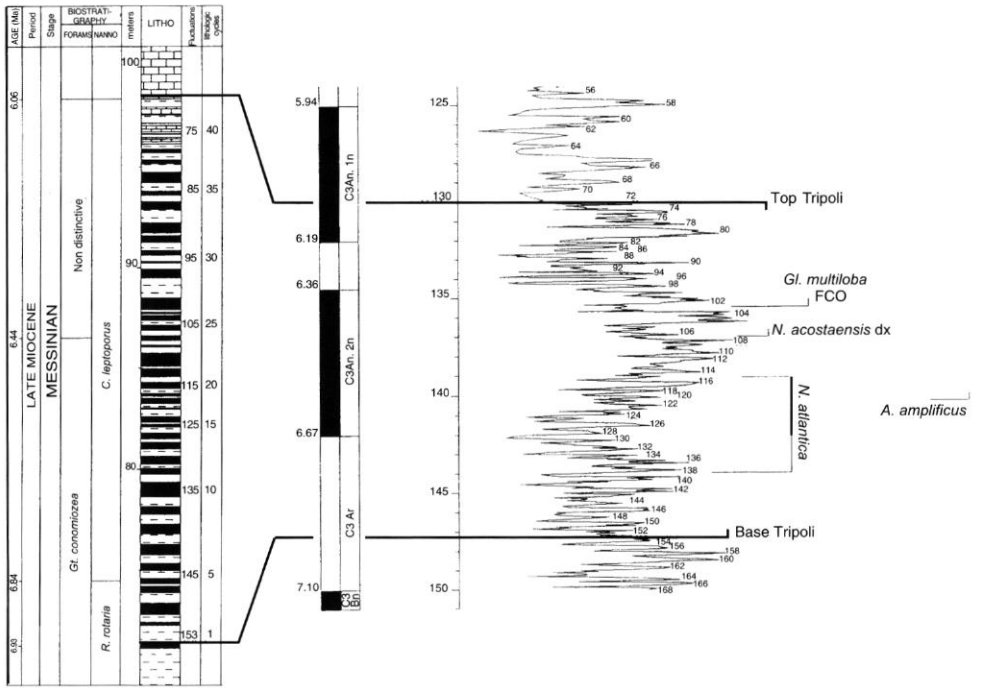

FIG. 2. — Correlation between Sprovieri *et al.* (1996) field-log for the Falconara Section, the polarity time-scale and the variations of the Cp/Rp (the two nannofossil species *Coccolithus pelagicus* and *Reticulofenestra pseudoumbilicus*) ratio at ODP Site 552. Selected bio-markers are also shown. Modified from Sprovieri *et al.* (1996).

rios to explain the cyclic diatomite formation as a result of: (1) the intensification of Atlantic inflow due to glacio-eustatic sea-level changes (Van der Zwaan & Gudjonsson 1986); (2) periodic upwellings (Gersonde 1980); (3) surface water warming (Broquet *et al.* 1981); (4) increased continental run-off (Meulenkamp *et al.* 1979); (5) global sea-level rise in combination with enhanced upwelling (McKenzie *et al.* 1979); (6) pulsating tectonics (Pedley & Grasso 1993).

With the uncertainty of the age of the Tripoli Formation and the exact origin of the cyclic bedding, Hilgen & Krijgsman (in prep.) conclude that the substitution of sapropel cycles by Tripoli diatomite cycles point to an orbital control on the sedimentary cyclicity, since sapropels are astronomically controlled (Hilgen *et al.* 1995; Sprovieri *et al.* 1996).

The palaeoclimatic interpretation of the diatomite-claystone couplets however, differs strongly from author to author. Sprovieri *et al.* (1996) suggest, based on planktonic foraminifers, that the deposition of claystones (or sapropels by some authors) took place during cold periods, while a warmer planktonic foraminifers assemblage is present in the diatomites. Müller (1985) concludes, based on nannofossil warm water species, that the claystones were deposited during warm periods, while diatomites reflect the influence of cold periods and upwelling. Hilgen & Krijgsman (1999) conclude that the diatomites (laminites) correspond to the precession minima and summer insolation maxima, and that the homogenous marls correspond to precession maxima and insolation minima.

The main goal of this paper is to examine the polycystine radiolarian fauna in the biosiliceous deposits in the Tripoli Formation as it outcrops at Falconara, Sicily (proposed by Colalongo *et al.* 1979) as a potential reference section for the Tortonian/Messinian boundary). The radiolarian

fauna is rich and well-preserved in most diatomites in the section and the radiolarian response to the cyclic changes are promising for a high-resolution biostratigraphic and correlation tool, as the radiolarian assemblages show major and significant changes between and within selected cycles (bulk radiolarian abundance, radiolarian flux, relative abundance of selected species, factor loadings, Spumellaria/Nassellaria ratio, etc.). These severe assemblage changes in the radiolarian fauna in the biosiliceous sediments at Falconara may provide information to improve and better understand the oceanographical and ecological evolution of the area.

STRATIGRAPHIC FRAMEWORK

In recent years Hilgen (1991), Langereis & Dekker (1992), Gautier *et al.* (1994), Suc *et al.* (1995), and Sprovieri *et al.* (1996) have been working on sediments of Messinian age in Sicily, while Hodell *et al.* (1994) worked up an age equivalent section in Morocco.

Hodell *et al.* (1994) convincingly demonstrated a high-resolution isotope, carbonate, magnetostratigraphic, and biostratigraphic record of a part of the Bou Regreg Section in north-western Morocco. The investigated drill core covered the time span from paleomagnetic Chron C4n partim to C3r (earliest Gilbert). This represents the time leading to and including the isolation and desiccation of the Mediterranean, i.e. the Messinian salinity crisis. They demonstrated that during Chrons C3An and C3Ar (6.935 to 5.894 Ma) the isotope and carbonate signals displayed a quasi-periodic variation with estimated periods of 40 and 100 kyr respectively. The *c.* 40 kyr period $\delta^{18}O$ signal was interpreted to reflect changes in the global ice volume caused by obliquity-induced changes (41 kyr period) in solar insolation in polar regions. They also concluded that the 100 kyr period carbonate variations were probably related to a long term modulation of the amplitude of the precessional cycle (*c.* 21 kyr period) which was not resolved due to their low sampling frequency.

The Falconara Section was first published by Catalano & Sprovieri (1971). D'Onofrio *et al.* (1975), Colalongo *et al.* (1979), van der Zwaan (1982), and Theodorites (1984) published on the calcareous plankton biostratigraphy in this section. Gersonde (1980) and Gersonde & Schrader (1984) reported on the diatom biostratigraphy, while stable oxygen and carbon isotope data were provided by van der Zwaan (1982), and van der Zwaan & Gudjonsson (1986).

Langereis *et al.* (1984), Hsü (1985), and Langereis & Dekker (1992) did not succeed in establishing a paleomagnetic stratigraphic framework for the section, while Gautier *et al.* (1994) claimed to have obtained paleomagnetic results from the Tripoli Formation.

Sprovieri *et al.* (1996) rejected the paleomagnetic results from Falconara proposed by Gautier *et al.* (1994). Instead they correlated the paleomagnetic record of ODP Site 552 (North Atlantic) with ODP Site 654 (Thyrrenian Sea), after having reinterpreted the magnetostratigraphic boundaries and their ages according to the magnetic polarity reversals record proposed by Cande & Kent (1992, 1995). The abundance fluctuations in the *Globigerinoides* sp. population at Site 654 were then correlated to the record of the same fluctuations in the Falconara Section.

ODP Site 552 from the North Atlantic was used by Sprovieri *et al.* (1996) to obtain the paleomagnetic boundary ages of Chron 3An by using the nannofossil abundance fluctuations published by Beaufort & Aubry (1990). Site 552 provides a complete sequence of abundance fluctuations (Fig. 2), forced by the astronomical precession cycles from the middle late Tortonian to the base of Zanclean. Sprovieri *et al.* (1996) were able to accurately correlate sedimentary and biostratigraphic events recorded in the Mediterranean basin with similar events in the North Atlantic (Site 552), and demonstrated that the ages could be estimated by comparison with the sequence of abundance fluctuations linked to the precession cycle. By this technique Sprovieri *et al.* (1996) estimated the base and top of the Tripoli Formation at Falconara to be 6.93 Ma and 6.08 Ma respectively (Fig. 2), which is the age model adopted in our present paper.

This deviates significantly from the age model provided by Hilgen & Krijgsman (in prep.).

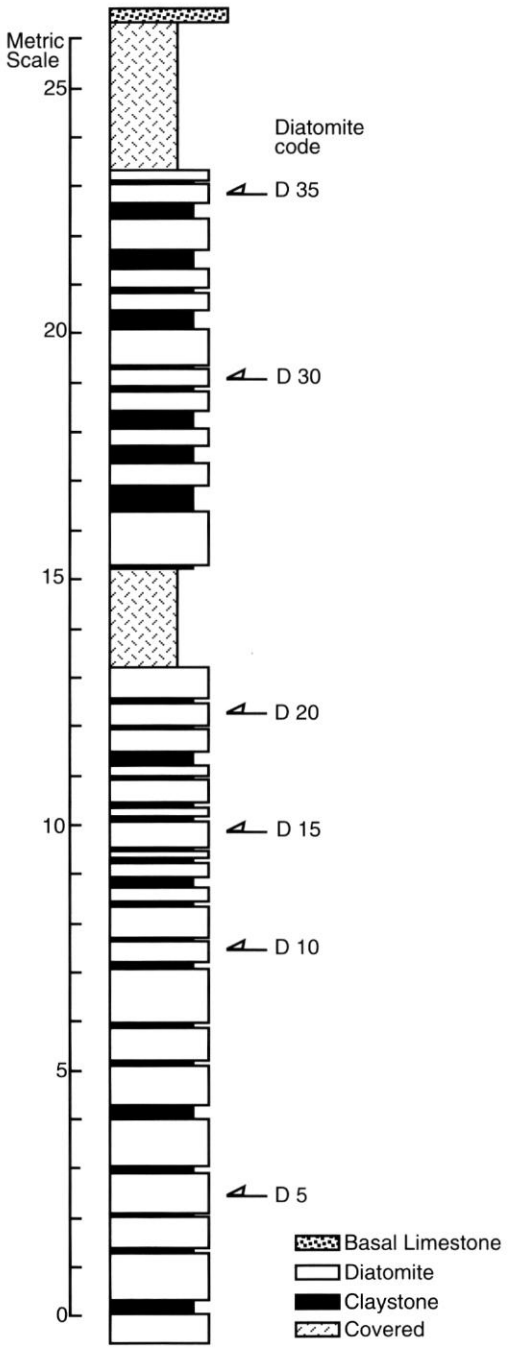

FIG. 3. — The 1995 field-log for the Falconara Section.

They used the position of the first and last occurrence of the planktonic foraminifer *Globorotalia nicolae* as the starting point for their tuning experiment. These events have been astronomically dated at 6.829 and 6.72 Ma in sections on Crete and Northern Italy (Hilgen *et al.* 1995; Krijgsman *et al.* 1997) and are located in the Tripoli cycle T9 and T14, respectively. With these ages as the starting point, all diatomite cycles have been tuned to the $La90_{(1,1)}$ precession and summer insolation time series (Hilgen & Krijgsman 1999). They provide absolute ages for all sedimentary cycles based on their astronomical calibration, resulting in 7.008 and 5.99 Ma for the base and the top of the Tripoli Formation. According to this new age model the Falconara Section starts with Tripoli cycle T8 (6.847 Ma) and contains 41 cycles (Hilgen & Krijgsman 1999), suggesting that Sprovieri *et al.* (1996) are missing seven Tripoli cycles. In future work, we will use the new age model of Hilgen & Krijgsman (1999). In Table 8 we have tabulated the sample ages according to Sprovieri *et al.* (1996) and indicated the correlation to the Tripoli cycles and absolute ages according to Hilgen & Krijgsman (1999).

MATERIAL AND METHODS

The study area covers the valley and hilly region delimited by the Sicani, Madonie and Erei Mountain Ranges (SW Sicily, Southern Italy), roughly coinciding to the Agrigento and Caltanissetta provincial territory (Fig. 1). Hitherto the best known Tertiary marine opal bearing sediments on Sicily are included in the Tripoli Formation, the so called diatomites or laminites, which are nicely exposed in the Falconara Section.

Our sampling program (May-June 1995 and August 1997) concentrated on the Messinian portion of the 27 m thick Falconara Section (Fig. 3). In 1995 we sampled a total of 30 out of 41 diatomites and 18 out of 41 claystones, (Table 2) and the remaining lithologies were sampled in 1997. The diatomites in Cycles 7, 21 and 28 were continuously sampled and are inclu-

ded in this work. The sampling of the Falconara Section resulted in two different sample sets: (1) one central sample per lithological unit for the 49 sampled lithologies; (2) one consisting in a continuous sampling of all the diatomites observed in the field. The maximum number of samples for a single diatomite was 48, resulting in a time-resolution of a few hundred years only.

In the Tripoli Formation Sprovieri *et al.* (1996) referred to the lithological levels and labelled the diatomites from T1 to T41 and the intercalated claystones from M1 to M42, with every negative or positive fluctuation in the nannoplankton flora representing a half-cycle. The claystones are arbitrarily assumed to represent the base of the cycles.

We have processed a total of 162 samples (Tables 2-5) from the Falconara Section and made slides for quantitative and qualitative analyses following the method proposed by Goll & Bjørklund (1974).

We selected the sample from the central part of each sampled lithological unit for both the diatomites and the claystones, assuming it to be representative for that lithology. All samples were analysed for their content of total organic carbon (TOC) and calcium carbonate by the use of an infrared gas analyser (LECO). This instrument measures, by infrared absorption, the amount of CO_2 released from the samples during combustion. The $CaCO_3$ content was calculated by the difference of C_{total} and $C_{carbonate\text{-}free}$ multiplied by the factor of 8.3 (atomic weight ratio of $CaCO_3$ to carbon).

Samples from within a single cycle have been coded, when plotted (Figs 7-12), as XX.YY [XX indicates the reference number for the cycle (Tables 3-5) and YY indicates the position of the sample within the cycle, given as a percentage of the time elapsed from the bottom of the cycle]. This has been done in order to simplify comparisons between different cycles, based on the assumption that the deposition of each cycle was influenced by the precession cycle, and therefore took place over an average time span of 21000 years (as demonstrated, for the Falconara Section, by Hilgen *et al.* 1995; Sprovieri *et al.* 1996). As a working hypothesis we had to assume that the sedimentation rate was constant throughout the cycle, in order to calculate

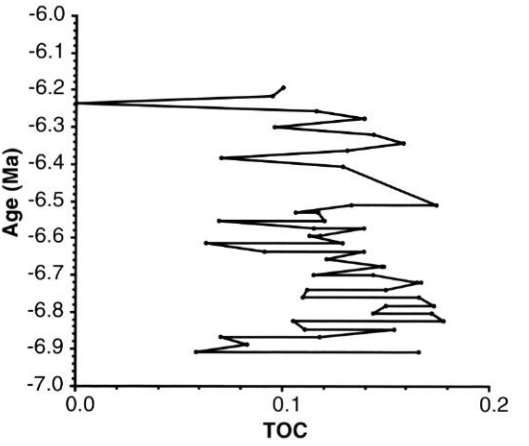

FIG. 4. — TOC (Total Organic Carbon) measurements through the section.

sample ages. Flux estimates are therefore based on the assumption that the deposition of each cycle took place over 21,000 years. These calculations were carried out on sediment cubes 2 × 2 × 2 cm.

The Factor Analysis Method (Imbrie & Kipp 1971) and the Fortran program CABFAC (Klovan & Imbrie 1971) were used for the statistical treatment of the data set. The Cabfac Q-Mode factor analysis program was used for grouping the samples in the Falconara Section into varimax assemblages based on the similarity between samples. This is done by transforming the raw data into variables (the factor components), each of which has a set of values (the varimax factor scores) giving an indication of which species are most important in each factor.

The species that were treated statistically had to occur as more than 2% of the total fauna in at least one sample, as recommended by Imbrie & Kipp (1971). This reduced the original 68 morphotypes (Table 1) counted during this study to 41 morphotypes used in the first factor analysis run. A selection of the morphotypes included in our factor runs are shown in Figs 20-22.

RESULTS

The organic carbon values from the central part

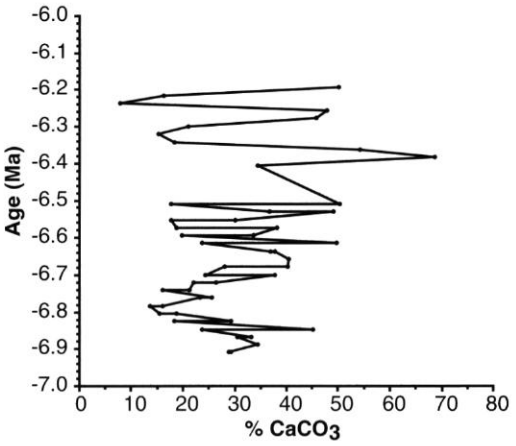

FIG. 5. — Percent of $CaCO_3$ through the section.

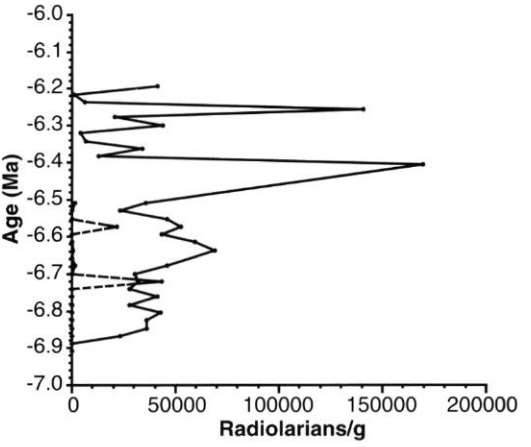

FIG. 6. — Number of radiolarians per gram bulk sediment in the diatomites through the section. Dashed line refers to claystones.

of the 49 lithologies (Table 2, Fig. 4) from Falconara are low, 0.06 < TOC < 0.18%, throughout the section. These low values are in good agreement with Brosse & Herbin (1990) who also reported on values much lower than 1% TOC in the upper Messinian of ODP Sites 654A and 652A in the Thyrrenian Sea. The $CaCO_3$ values (Table 2, Fig. 5) show fluctuations between 7.92 and 50.09%.

The abundance of radiolarian specimens in the 49 studied lithologies ranges from zero in Cycle 2 till more than 169000 radiolarians/g bulk sediment in Cycle 26 (Fig. 6), therefore indicating that the different cycles display marked variations in the total abundance of radiolarian specimens and in the species composition as demonstrated by the changes in factor loadings, as we will show later (Figs 15-19, Tables 6-8).

Our data show that radiolarians are usually not present in the claystones (Table 2, Fig. 6), as also documented for the diatoms (Gersonde 1980; Gersonde & Schrader 1984). Of our 19 claystones, nine were barren for polycystine radiolarians, while eight had low numbers, less than 3,000 radiolarians/g carbonate free sediment. However, two claystones had significant high numbers, more than 43,000 (S11) and about 21,500 (S18) radiolarians/g bulk sediment.

The abundance of radiolarian skeletons is showing great changes between the different diatomites (Fig. 6). To test how the radiolarian abundance changed within a cycle and between cycles, we arbitrarily selected three continuously sampled diatomites, the lowest at *c.* 5 m, the middle at *c.* 12 m and the uppermost at *c.* 18 m into the section, respectively:

Cycle 7. (Figs 7, 10; Table 3): diatomite D7, in the lower part of the section, is 46.9 cm thick and the claystone/diatomite boundary is 46.6% into the cycle. This percentage notation has been adopted in order to have a way to directly compare the data obtained from different cycles, with the assumption that the sedimentological evolution of each cycle is the same.

Cycle 21. (Figs 8, 11; Table 4): diatomite D21, in the middle of the section, is 64 cm thick and the claystone/diatomite boundary is about 11% into the cycle.

Cycle 28. (Figs 9, 12; Table 5): diatomite D28, in the upper part of the section, is 49.7 cm thick and the claystone/diatomite boundary is about 49.2% into the cycle.

In the three cycles chosen in this experiment, the abundance of radiolarians varies between *c.* 3,200 in Cycle 28 and *c.* 117,000 radiolarians/g bulk sediment in Cycle 7. We have no calcium carbonate data for the continuous sampled diatomites but the variation patterns of the radiolarian abundance number within the three cycles are however distinct (Figs 7-9).

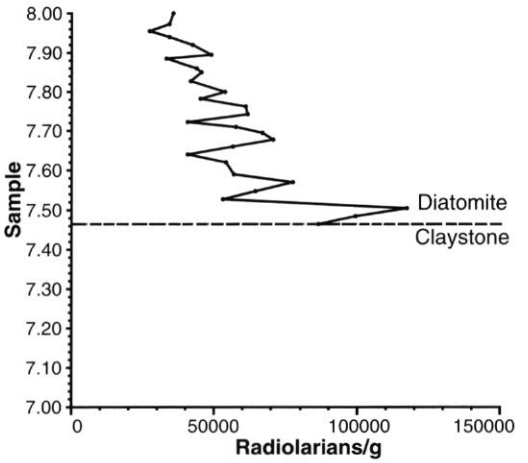

FIG. 7. — Number of radiolarians per gram bulk sediment through Cycle 7. The dashed horizontal line marks the transition between claystone and diatomite.

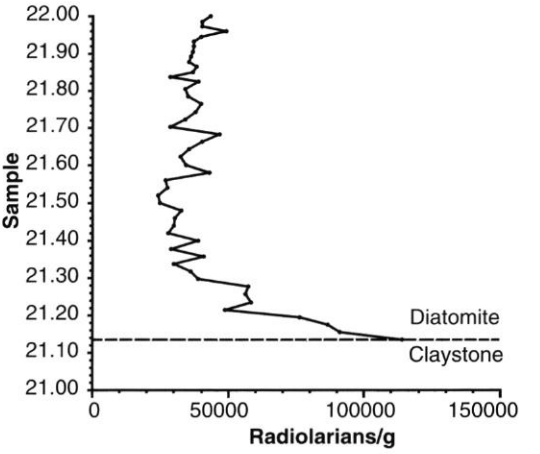

FIG. 8. — Number of radiolarians per gram bulk sediment through Cycle 21. The dashed horizontal line marks the transition between claystone and diatomite.

In the following we will discuss only the diatomites from the three selected cycles.

Cycle 7. Radiolarians are present with highest abundances (Fig. 7) in the lower 10% of the diatomite (*c.* 117,000 radiolarians/g bulk sediment), while the number gradually decreases towards the top of the diatomite (*c.* 27,200). As can be seen from the Spumellaria/Nassellaria (S/N) ratio, spumellarians are dominating over nassellarians in the bottom five samples (with one exception), while in the rest of the diatomite the S/N ratio fluctuates around a value of 0.7, indicating a dominance of nassellarians (Fig. 10).

Cycle 21. Radiolarians are present with highest abundances in the lower 10% of the diatomite (*c.* 114,000 radiolarians/g bulk sediment). This number rapidly decreases to *c.* 40,000 *c.* 20% into the diatomite, thereafter it fluctuates from between *c.* 24,000 and 49,000 towards the top (Fig. 8). In the lower 15% of the diatomite (with the exception of the oldest sample), the S/N ratio is higher than one, while for the remaining part of the diatomite nassellarians are the dominant group (Fig. 11).

Cycle 28. Radiolarians are present with highest abundances in the lower 10% of the diatomite (*c.* 55,000 radiolarians/g bulk sediment). This number rapidly decreases to less than 10,000 *c.* 15% into the diatomite, thereafter it remains almost constant (Fig. 9). In this diatomite the spumellarians are dominant throughout, in contrast to the previous two cycles, where nassellarians are the dominant group. In the topmost 20% of the diatomite the S/N ratio fluctuates between 10 and 65 (Fig. 12).

In order to take the dilution effect of carbonate into consideration we plotted the number of radiolarians/g carbonate free sediment of the central sample from all lithologies (Fig. 13). We have sampled 19 out of 41 claystones and only two have a significant radiolarian content, between 30,000 and 50,000 radiolarians/g carbonate free sediment, while two diatomites have values reaching more than 250,000 radiolarians/g carbonate free sediment.

The distorting effect of the (most likely changing) sedimentation rate through the section was then considered, and we calculated a radiolarian flux curve for the section (Fig. 14), accepting the diatomites and claystones to be precession controlled, with an average duration of 21.000 years. This curve depicts the changes of the number of radiolarians per time- and per surface-unit (e.g., number of radiolarians/kyear/cm^2), thus being an image of the changes in radiolarian productivity through time, which is independent both from the composition and

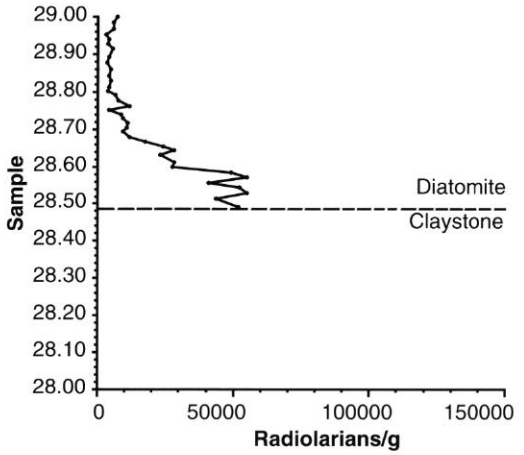

FIG. 9. — Number of radiolarians per gram bulk sediment through Cycle 28. The dashed horizontal line marks the transition between claystone and diatomite.

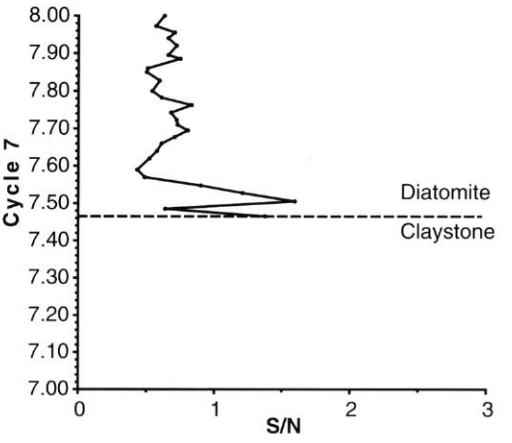

FIG. 10. — S/N ratio through Cycle 7. The dashed horizontal line marks the transition between claystone and diatomite.

from the accumulation rate of the sediment hosting the microfossils. It is apparent that only one diatomite (D26) represents one major high production pulse with an outstanding radiolarian flux (304,000 radiolarian skeletons/kyear/cm^2) when compared to the rest of the diatomites (Fig. 14; Table 2). This abundance peak is a potential event to be used as a key-level in local and regional correlation.

The application of Q-mode factor analysis to a total of 41 morphotypes resulted in 10 factors (polycystine radiolarian associations), explaining a cumulative variance of 95.89% (data from this run are not presented herein). The 13 morphotypes having a varimax factor component value higher than 2.000 (i.e. the most "important" species for each factor) in this run were then used once again in a second factor analysis run. The results between the two runs are not significantly different, therefore enabling us to work with only 13 rather than the 68 morphotypes that we started out with. This reduction in species will speed up the counting time, and this technique can, therefore be a potentially useful tool for correlation. The screening (the first factor run) and reduction to only the 13 most important morphotypes will make it easier to compare and use data from other authors. Of the factor component peaks resulting from this run we tabulated in Table 8, 46 factor component values higher than 0.400 (Table 6).

Factor 1 (dominated by the *S. delmontensis* group, Table 7) reaches high values in different portions of the section, but is more significant in sediments older than 6.50 Ma (Fig. 15).

Factor 2 (dominated by Larcoidea sp., Table 7) is common throughout the section becoming more important in sediments younger than 6.54 Ma (Fig. 16).

Factor 3 (dominated by *Lithomitra lineata*, Table 7) is the only factor that gives a good opportunity to split the Falconara Section in a higher and lower portion, as high values for this factor are only found in the lower portion of the section, in sediments older than 6.60 Ma (Fig. 17).

Factor 4 (dominated by *Didymocyrtis* sp., Fig. 18; Table 7) is one factor assigned to the claystones, peaking in S13 and S16. On the quantitative slide of sample S16 no radiolarians were found (Table 2), however, on the enriched fauna slides an almost monospecific *Didymocyrtis* sp. assemblage occurred.

Factor 7 (dominated by *Anthocyrtidium ehrenbergi*, Fig. 19; Table 7) is the second factor assigned to the claystones with one peak in S21.

DISCUSSION

The Falconara Section is peculiar in its radiolarian assemblage and species morphology. These

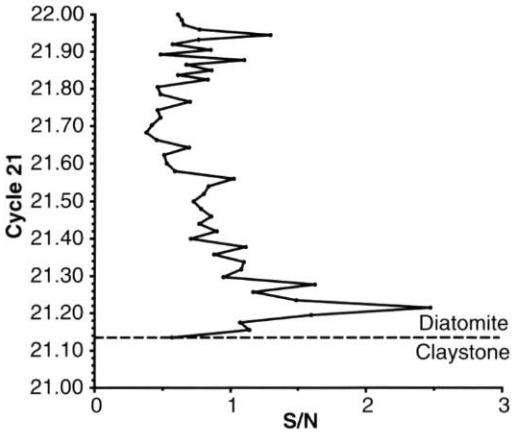

FIG. 11. — S/N ratio through Cycle 21. The dashed horizontal line marks the transition between claystone and diatomite.

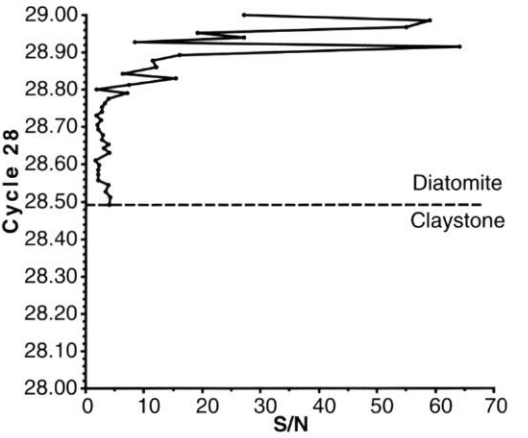

FIG. 12. — S/N ratio through Cycle 28. The dashed horizontal line marks the transition between claystone and diatomite.

deposits are immediately pre-dating the isolation and desiccation of the Mediterranean Sea, causing "stressed" ecological conditions for the plankton. The following scenarios have been used to explain the cyclic diatomite formation, events that can also cause these stressed ecological conditions: (1) the intensification of Atlantic inflow due to glacio-eustatic sea-level changes (Van der Zwan & Gudjonsson (1986); (2) periodic upwellings (Gersonde 1980); (3) surface water warming (Broquet *et al.* 1981); (4) increased continental run-off (Meulenkamp *et al.* 1979); (5) global sea level rise in combination with enhanced upwelling (McKenzie *et al.* 1979); (6) pulsating tectonics (Pedley & Grasso 1993). Hilgen & Krijgsman (1999) point out that the Miocene sapropels had the same origin as the Pliocene-Pleistocene ones, namely dominantly precession controlled "dry-wet" oscillations in the circum-Mediterranean climate. These alternations certainly caused differences in the living conditions for the marine microplankton.

The age of the Tripoli Formation exposed in the Falconara Section was determined by Hilgen & Krijgsman (1999) to range from 6.847 to 5.980 Ma, starting with Tripoli Cycle T8, compare Sprovieri *et al.* (1996) giving the range of 6.93 to 6.08 Ma, corresponding to the nannofossil *C. leptoporus* zone. The standard radiolarian zonation cannot directly be applied to the Mediterranean Sea, nor to the Messinian siliceous deposits on Sicily.

The base of the radiolarian *Stichocorys peregrina* zone is defined as the transition from *S. delmontensis* to *S. peregrina*, dated to occur at *c.* 6.2-6.3 Ma (Theyer & Hammond 1974). Riedel *et. al.* (1974) reported on one radiolarian-rich sample in the Trubi marls of the Capo Rossello, assigned to the Zanclean stage, lower Pliocene, stating: "...the "Trubi" assemblage is to be placed between the time of evolutionary transition from *S. delmontensis* to *S. peregrina*, and that from *Spongaster berminghami* to *S. pentas*, and thus evidently belongs to the *Stichocorys peregrina* zone." From the same profile Riedel & Sanfilippo (1978) also report on common typical oceanic specimens of *S. peregrina* with truncated-conical third segment.

In the Falconara Section, assigned to the older Tripoli Formation, we have not been able to observe this transition. We include in the *S. delmontensis* group several morphologies, some with a thick silicified test, others with a very thin test, and several forms having irregularly shaped segments with tilted strictures between segments. No real specimens of the oceanic form of *S. peregrina* have been observed in our material. We therefore assign the section to predate the *Stichocorys peregrina* zone.

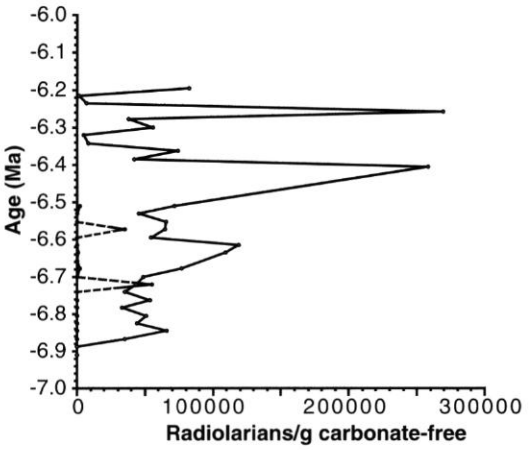

FIG. 13. — Number of radiolarians per gram $CaCO_3$-free in the diatomites through the section. Dashed line refers to claystones.

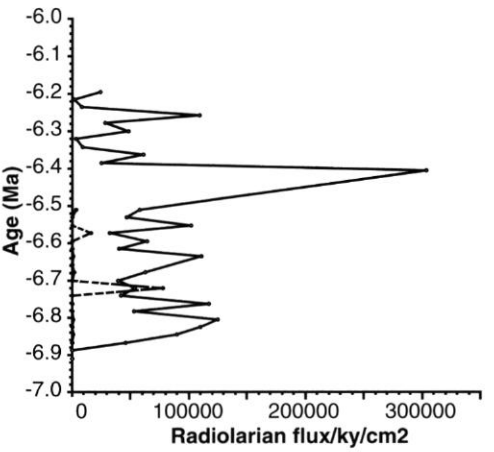

FIG. 14. — Radiolarian flux (number of radiolarians/kyear/cm^2) through the section. Dashed line refers to claystones.

Foraminiferal assemblages are generally present in the diatomites with a rich and diversified fauna, while the diversity is generally lower in the claystones. In some claystone units the foraminiferal assemblages are missing, e.g., M30, M41, and M42 (Sprovieri *et al.* 1996). They suggest that the claystones are deposited during cold periods while the diatomites are deposited during warm periods, as they generally have a warmer planktonic foraminifer assemblage.

Müller (1985) on the other hand concludes the opposite. The claystones have a higher amount of nannoplankton and a more diversified assemblage with input of warm water species (i.e. *Sphenolithus abies*) and some discoasters. She therefore concluded that the claystones were deposited during warm periods, while the diatomites were formed during cold periods and times with upwelling related to changes in the prevailing wind direction.

The *Sticochorys delmontensis* group is present throughout the section and varies greatly in abundance as well as morphology, as also observed in the Gibliscemi Section (Caulet pers. comm. 1997). The variation in the skeletal morphology in the *S. delmontensis* group is a potential tool in interpreting the paleoclimate if we can decode the meaning of these variations.

The *S. delmontensis* association (Factor 1, Fig. 15) and *Lithomitra lineata* association (Factor 3, Fig. 17) show almost the same pattern of major and rapid variations in the lower part of the section, older than 6.5 Ma, interpreted as rapid ecological changes over very short time intervals.

In Factor 2 Larcoidea sp., *Porodiscus* sp., and *Spongotrochus glacialis* are the dominant taxa, after 6.5 Ma and modern equivalents of these categories are often found in deeper and cooler water, except for *Stylochlamidium venustum* (forms that we included in the *Porodiscus* sp.) showing a shallow and warm water affinity in the Pacific (Mullineaux & Westberg-Smith 1986). As the modern equivalents of these groups do refer to open ocean conditions, it is not easy to interpret the Falconara Section in a scenario where the shallow Caltanissetta basin has a restricted communication with the ocean.

Diatoms are generally absent or badly preserved in the claystones (Gersonde 1980; Gersonde & Schrader 1984). Similarly for the radiolarians, but two claystones have significant amounts of radiolarians, S18 (21,500 radiolarians/g bulk sediment) and S11 (43,000 radiolarians/g bulk sediment). In addition three claystones are characteristic by their fauna associations, S13 and S16 (by Factor 4, dominated by *Didymocyrtis* sp.) and S21 (by Factor 7, dominated by *Anthocyrtidium ehrenbergii*). These five levels are potential good local or regional markers within the Caltanissetta basin.

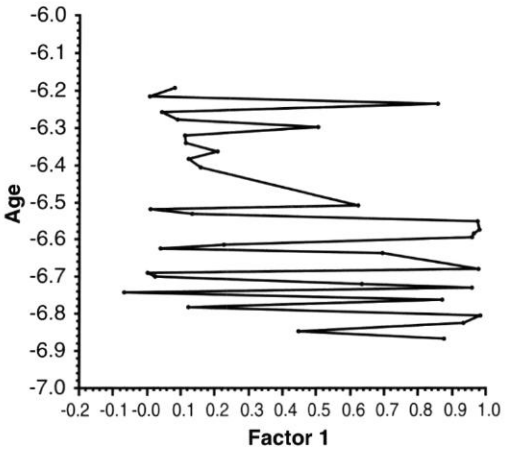

FIG. 15. — Factor components through the section (Factor 1).

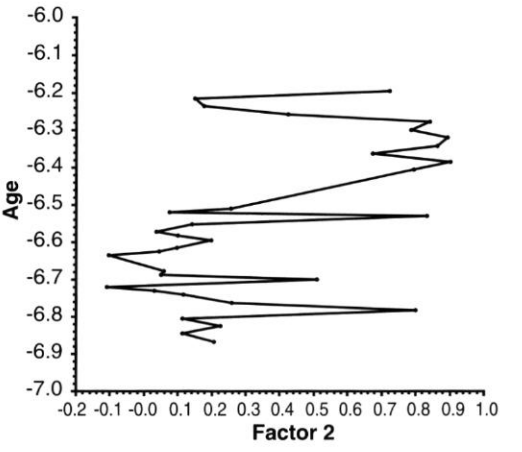

FIG. 16. — Factor components through the section (Factor 2).

The *Didymocyrtis* sp. is almost monospecific and as the section is predating the *Stichocorys peregrina* zone, the *Didymocyrtis penultima* zone would seem natural, but we cannot assign our assemblage to this zone with certainty. This form of *Didymocyrtis* sp. might be the oceanic counterpart of *Didymocyrtis penultima*, however, it differs so much that it probably is a new species. We do not think that this morphology is simply a result of different ecology and corresponding ontogenesis.

The diatomites show great variation in the number of radiolarians/g sediment, both between the different diatomites and within them (Figs 6-9). To test the hypothesis if there is a rhythmic development through time between the different diatomites, we assigned each sample to its time equivalent position within each cycle, assuming a claystone and a diatomite couplet to represent 21,000 years. Each claystone and diatomite has its own polycystine radiolarian "fingerprint" (assemblage or event) as determined by the percent distance into the cycle. This will provide an excellent stratigraphic tool with a high and precise time resolution (Table 8).

Another "fingerprint" that can help to recognise the different diatomites is the Spumellaria/Nassellaria (S/N) ratio. D7 and D21 show a very similar and systematic evolution in this ratio, where spumellarians dominate the lower part of the cycle, while the nassellarians take over in the upper part of these cycles (Figs 10-11). D28 shows a different trend in the Spumellaria/Nassellaria ratio since the spumellarians are always dominant and they become much more so in the upper part of the cycle (Fig. 12).

The differences in the polycystine radiolarian "fingerprint" between cycles cannot be explained at present, but only speculated upon. The microfauna of the Tripoli Formation, both at Capodarso (Suc *et al.* 1995) and at Falconara (Sprovieri *et al.* 1996) is rich in planktonic foraminifera, a typical oceanic imprint. The sedimentation history of the Caltanissetta basin has changed through the Messinian, as documented by the alternation of diatomites and claystones due to processes causing the isolation, changes in production and preservation of organic material, changes in primary and secondary production, and desiccation of the basin, compare the scenarios outlined elsewhere. Suc *et al.* (1995) point out that the diatomite-claystone couplets are a result of sea-level fluctuations. Sprovieri *et al.* (1996) on the other hand concluded that the rhythmites are astronomically forced due to the 21,000 yrs periodicity based on the occurrence of planktonic foraminifers, as also supported by Hilgen *et al.* (1995) and Hilgen & Krijgsman (1999).

Whatever causes the rhythmites, the presence or

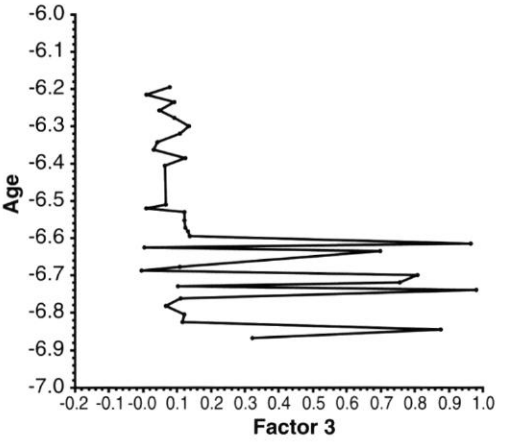

FIG. 17. — Factor components through the section (Factor 3).

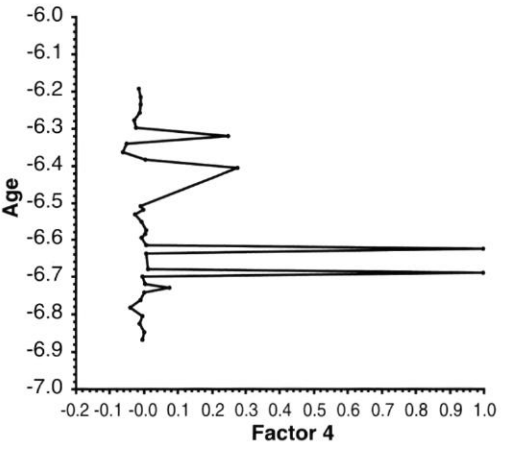

FIG. 18. — Factor components through the section (Factor 4).

absence of polycystine radiolarians is a result of changes in the ecological, as well as in the preservational conditions within the Caltanissetta Basin. Suc *et al.* (1995) concluded that the Contrada Gaspa Section, constituted by 108 m of sediments ranging from diatomites to clayey diatomites, was a result of deposition in a small basin intermittently isolated from the Caltanissetta Basin. The Falconara Section, near to the rim of the Caltanissetta Basin, has a different lithological structure than the Capodarso Section, therefore making correlations difficult.

This makes the Caltanissetta basin an analogue to modern Norwegian fjords. Polycystine radiolarians have been shown (Swanberg & Bjørklund 1986, 1987) to live and thrive in very landlocked environments such as fjords and polls, where they occur in the plankton in concentrations of *c.* 10000 radiolarians/m^3 seawater. In one poll the assemblage is almost monospecific (*Amphimelissa setosa*) showing a different skeletal morphology than the oceanic counterpart period Bjørklund & Swanberg (1987) suggested that in the warm end of its temperature range, in the fjords, the availability of nutrition gave a much higher growth rate that resulted in smaller and reticulated forms, while the oceanic forms, in the cold end of its temperature range, grew slower and over a longer time period, resulting in a larger and more silicified skeleton with rounded pores. An analogue is the *S. delmontensis* in the Caltanissetta Basin which shows a big variation in its morphology, where we identified and counted four different morphotypes. It is apparent that in certain parts of the section, and even in certain parts within the single diatomites, the different morphologies of *S. delmontensis* must be a response to ecological changes. The "dry-wet" oscillations in the Mediterranean climate and the enhanced continental run-off (Meulenkamp *et al.* 1979) must certainly be kept in mind.

The high neritic plankton values are in conflict with the general understanding that radiolarians are not abundant in the neritic environments. In the fjord sediments 1,000 polycystine radiolarians/g is a normal value, as the terrigenous input due to river discharge is high and the microfossil remains are very much diluted.

The Caltanissetta Basin, if compared with a fjord situation, must be of a different magnitude and structure. Terrigenous sediments must be trapped in near land "sub-basins" with the possibility to produce, accumulate and preserve biogenic sediments rich in both carbonate and opal microfossil remains, probably the Caltanissetta basin was more open than the analogue fjords.

High levels of organic material and opal microfossils are, however, deposited in present day anoxic basins such as in the Tyro Basin in the eastern Mediterranean (Bjørklund & de Ruiter

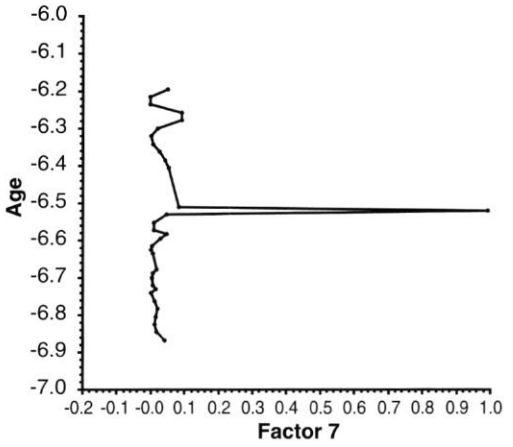

FIG. 19. — Factor components through the section (Factor 7).

1987) in contrast to the oxygenated sediments in the Mediterranean proper (Caulet 1974) which are poor in opal microfossils.

The Spumellaria/Nassellaria ratio has been used as a potential tool to discriminate between assemblages in neritic environments (Palmer 1986) where spumellarians predominate the plankton, *vs* open oceanic environments where nassellarians tend to be the dominant group (McMillan 1979, 1981). Swanberg & Bjørklund (1987) clearly demonstrated that the radiolarian fauna of Sogndalsfjorden was dominated by early developmental stages of *Amphimelissa* sp. which comprised 11%, 39% and 60% of the plankton fauna proceeding from the outer to the inner fjord basin. In two other landlocked basins the same species made up 91 and 99% of the fauna. This clearly demonstrates the occurrence of nassellarians with more than 99% in the neritic plankton, in opposition to the conclusions by Palmer (1986) and McMillan (1979, 1981), and does not signal open ocean conditions.

If our detailed investigation of the S/N ratio in the three different cycles (Figs 10-12) should be interpreted as depicting neritic and oceanic conditions, both D7 and D21 would then show a gradual evolution from neritic to oceanic conditions as they are dominated by spumellarians close to the base of the diatomites, while nassellarians are increasing towards the top. The S/N ratio in D28 suggests on the contrary that this cycle was exclusively deposited in a neritic environment. We cannot see any direct connection between the S/N ratio and the neritic *vs* oceanic environments (distance from shore), as interpreted by Palmer (1986). The change in the S/N ratio is more subject to local ecological changes within the basin, and not so much a result of the sites position in relation to the coast or the open oceanic. Boltovskoy (pers. comm. 1997) also observed that the S/N ratio behaves inconsistently on different sediment types.

Our conclusion is therefore that the S/N ratio in the sediment cannot be used to discriminate between neritic *vs* oceanic conditions, mostly as this ratio is very sensitive to dissolution, a common problem in the hemipelagic province. Locally, however, the S/N ratio can be a useful stratigraphic tool to recognise polycystine distribution patterns, both within and between cycles in a section, as well as between sections. This because the S/N ratio in this scenario probably depicts changes and differences in the ecology and in the production, as well as in the accumulation and preservation conditions of microfossils.

The diatomites are generally very rich in radiolarians and we tend to conclude that nutrient availability in the basin during their formation is good, probably as a result of continental run off (Meulenkamp *et al.* 1979). The almost total lack of planktonic life in the claystone lithologies in the Capodarso Section (Suc *et al.* 1995) indicates that the absence of siliceous microfossils is not only a result of silica dissolution. Also planktonic foraminifers are absent or rare, while the benthic foraminifer fauna is restricted (Suc *et al.* 1995), indicating that an environmental stress is affecting the basin. The micro lamination do indicate periodic anoxic conditions.

Particularly high values of the factor component peaks for the final nine factors (higher than 0.400, framed in Table 6) were used to trace the most important "radiolarian factor peaks" throughout the section. The peaks (Table 8) are coded as X.Y, where X represents the factor number and Y represents a reference number for the "factor peaks", arranged in an ascending order from base to top of the section.

Some factors (Table 8, e.g., Factor 1) display "16

factor peaks" (framed values in Table 6) in different portions of the section (e.g., from diatomites D4 to D34), which have to be interpreted as the recurrence of equivalent ecological or hydrographical conditions at different times.
The peak pattern as presented in Table 8, is our first attempt to make a radiolarian stratigraphic synthesis of the Falconara Section based on "factor peaks", and the peak order obviously represent an evolution of the radiolarian assemblage as a response to changing environments. To use the peaks as a correlation tool between our reference section (Falconara) and another section we have to pick a sequence of factor peaks from the section we want to correlate and look for the same peak pattern in the reference section. We see this technique to be especially useful when correlating profiles in the same section where visual correlation is difficult due to tectonism.

CONCLUSIONS

1. In diatomites the number of radiolarians/g bulk sediment fluctuates between 1,200 (D35) and 169.500 (D26). One diatomite (D2) is barren.
2. On a $CaCO_3$ free basis, D26 has a flux of 303,500 radiolarian skeletons/kyear/cm^2. A possible regional marker for correlation.
3. In D7 and D21 spumellarians are dominant in the lower 10-15% of the diatomites, while nassellarians dominate the upper part.
4. In D28 spumellarians dominate the whole diatomite.
5. The S/N ratio reflects local ecological changes (as shown in D28).
6. In claystones the number of radiolaria/g bulk sediment is generally barren or low. Two claystones, S18 and S11, have high numbers of 21,500 and 43,000, respectively, and may serve as a correlation tool.
7. S13 and S16 have factor component peaks of 0.997 and 0.997 respectively, two claystones that may serve as a regional marker, dominated by an almost monospecific *Didymocyrtis* sp. (not *Didymocyrtis penultima*) assemblage.
8. S21 has a factor component peak of 0.993, *Anthocyrtidium ehrenbergii* is the important species, and may be a stratigraphical marker.

Acknowledgements
We are thankful to Dr. J. P. Caulet who reviewed and made comments that greatly improved the manuscript.
Dr. G. Cortese would like to thank the following institutions for the economic support during the realisation of the manuscript: the Paleontological Museum (University of Oslo), the Norwegian Research Council (KAS fellowship) and the Norwegian Academy of Sciences through the program "Nansenfondet og de Dermed forbundne fond".
Prof. K. R. Bjørklund would acknowledge the support and inspiration provided by Dr. M. Marcucci, Dipartimento Scienze della Terra, Florence, Italy. We are thankful to Dr. H. A. Nakrem for the support and facilities provided by the Paleontological Museum, and for his inspiration and practical help during this work. This is the Contribution number 415 from the Paleontological Museum, University of Oslo.

REFERENCES

Beaufort L. & Aubry M. P. 1990. — Fluctuations in the composition of late Miocene calcareous nannofossil assemblages as a response to orbital forcing. *Paleoceanography* 5(6): 845-865.
Bjørklund K. R. 1976. — Radiolaria from the Norwegian Sea, Leg 38 of the Deep Sea Drilling Project: 1101-1168. *in* Talwani M., Udintsev G. (eds), *Initial Reports of the Deep Sea Drilling Project* 38. U.S. Governmental Printing Office, Washington D.C.
Bjørklund K. R. & Swanberg N. R. 1987. — The distribution of two morphotypes of the radiolarian *Amphimelissa setosa* Cleve (Nassellarida): A result of environmental variability ? *Sarsia* 72: 245-254.
Bjørklund K. R. & de Ruiter R. 1987. — Radiolarian preservation in estern Mediterranean anoxic sediments. *Marine Geology* 75: 271-281.
Broquet P., Mascle G. & Monnier M. 1981. — La formation à tripolis du bassin de Caltanissetta (Sicile). *Revoe de géologie dynamique et géographie physique* 25 : 87-98.
Brosse E. & Herbin J. P. 1990. — Organic geochemistry of ODP Leg 107 sediments (Sites 652, 653, 654, 655). *in* Kastens K. A., Mascle J. *et al.* (eds), *Proceedings of the Ocean Drilling Project, Scientific Results* 107: 537-544.
Butler R. W. H., Lickorish W. H., Grasso M., Pedley H. M. & Ramberti L. 1995. — Tectonics and sequence stratigraphy in Messinian basins, Sicily:

Constraints on the initiation and termination of the Mediterranean salinity crisis. *Geological Society of America, Bulletins* 107: 425-439.

Cande S. C. & Kent D. V. 1992. — A new geomagnetic polarity timescale for the late Cretaceous and Cenozoic. *Journal of Geophysical Research* 97: 13917-13951.

— 1995. — Revised age calibration points for the geomagnetic polarity time scale. *Geophysical Research Letters* 22: 957-960.

Catalano R. & Sprovieri R. 1971. — Biostratigrafia di alcune serie saheliane (Messiniano inferore) in Sicilia: 211-249, *in* Farinacci A. (ed.), *Proceedings of the II Planktonic Conference, Roma 1970.*

Caulet J.-P. 1974. — Les radiolaires des boues superficielles de la Méditerranée. *Bulletin du Muséum national d'Histoire naturelle*, serie 3, n° 249, juillet-août 1974, Sciences de la Terre 39 : 217-288.

Cocco L. 1905. — I Radiolari fossili del tripoli di Condro′ (Sicilia), in *Rendiconti e Memorie della Regia Accademia di Scienze, Lettere ed Arti degli Zelanti* (Acireale), Serie 3, Vol. III, Memorie della Classe di Scienze: 1-14.

Colalongo M. L., Di Grande A., D'Onofrio S., Giannelli L., Iaccarino S., Mazzei R., Romeo M. & Salvatorini G. 1979. — Stratigraphy of Late Miocene Italian sections straddling the Tortonian/Messinian boundary. *Bollettino della Societa' Paleontologica Italiana* 18: 258-302.

D'Onofrio S., Giannelli L., Iaccarino S., Morlotti E., Romeo M., Salvatorini F., Sampò M. & Sprovieri R. 1975. — Planktonic foraminifera of the Upper Miocene from some Italian sections and the problem of the lower boundary of the Messinian. *Bollettino della Societa' Paleontologica Italiana* 14: 177-196.

Dumitrica P. 1973. — Cretaceous and Quaternary Radiolaria in deep sea sediments from the northwest Atlantic Ocean and Mediterranean Sea. *Initial Reports of the Deep Sea Drilling Project*, U.S. Government Printing Office 13 (2): 829-901.

Ehrenberg C. G. 1854. — *Mikrogeologie.* XXVIII + 374 p., Atlas 31 p., 40 pls., *Fortsetzung* (1856), 88 p. + 1 p. [errata]. Voss, Leipzig.

Gautier F. 1994. — *Calibration magnetostratigraphique du Messinien de la Méditerranée occidentale. Age, durée et déroulement de la crise de salinité.* Doctorat thesis, Université Montpellier II, Science et Techniques du Languedoc, 152 p.

Gautier F., Clauzon G., Suc J. P., Cravatte J. & Violanti D. 1994. — Age et durée de la crise de salinité messinienne. *Comptes Rendu de l'Academie des Sciences*, Paris 318 : 1103-1109.

Gersonde R. 1980. — *Paläoökologische und Biostratigraphische Auswertung von Diatomeen Assoziation aus dem Messinium aus dem Caltanisetta-Beckens (Sizilien) und einiger Vergleichs-Profile in SO-Spanien, NW Algerien und auf Kreta.* Thesis, Universität Kiel, 393 p.

Gersonde R. & Schrader H. 1984. — Marine planktic diatom correlation of Lower Messinian deposits in the western Mediterranean. *Marine Micropaleontology* 9: 93-110.

Goll R. M. & Bjørklund K. R. 1974. — Radiolaria in surface sediments of the South Atlantic. *Micropaleontology* 20(1): 38-75.

Hilgen F. 1991. — Extension of the astronomically calibrated (polarity) time scale to the Miocene/Pliocene boundary. *Earth and Planetary Science Letters* 107: 349-368.

Hilgen F. & Krijgsman W. 1999 — Cyclostratigraphy and astrochronology of the Tripoli diatomite Formation (pre-evaporite Messinian, Sicily, Italy). *Terra Nova* 11: 16-22.

Hilgen F., Krijgsman W., Langereis C. G., Lourens L. J., Santarelli A. & Zachariasse W. J. 1995. — Extending the astronomical (polarity) time scale into the Miocene. *Earth and Planetary Science Letters* 136: 495-510.

Hodell D. A., Benson R. H., Kent D. V., Boersma A. & Rakic-El Bied K. 1994. — Magnetostratigraphic, biostratigraphic, and stable isotope stratigraphy of an Upper Miocene drill core from the Salé Briqueterie (northwestern Morocco): a high-resolution chronology for the Messinian stage. *Paleoceanography* 9(6): 835-855.

Hollande A. & Enjumet M. 1960. — Cytologie, Évolution et Systématique des Sphaeroïdés (Radiolaires). *Archives du Muséum national d'Histoire naturelle,* Série 7, VII : 1-134.

Hsü K. J. 1985. — Unresolved problem concerning the Messinian salinity crisis. *Giornale di Geologia* 47: 203-212.

Imbrie J. & Kipp N. G. 1971. — A new micropaleontological method for quantitative paleoclimatology: application to a late Pleistocene Caribbean core: 71-147, *in* Turekian K. K. (ed.), *The late Cenozoic glacial ages*. Yale University Press, New Haven-London.

Jørgensen E. 1905. — The protist plankton and the diatoms in bottom samples, *in* Nordgaard O. (ed.), Hydrographical and biological investigations in Norwegian fjords, *Bergens Museums Skrifter* 1 (7): 49-151.

Klovan J. E. & Imbrie J. 1971. — An algorithm and FORTRAN-IV program for large-scale Q-mode factor analysis and calculation of factor scores. *Journal of the Indian Society of Soil Science* 3 (1): 61-77.

Krijgsman W., Hilgen F. J., Negri A., Wijbrans J. R. & Zachariasse W. J. 1997. — The Monte del Casino section (northern Apennines, Italy): A potential Tortonian/Messinian boundary stratotype? *Palaeogeography, Palaeoclimatology, Palaeoecology* 133: 27-47.

Langereis C. G. & Dekker M. J. 1992. — Paleomagnetism and rock magnetism of the Tortonian-Messinian boundary stratotype at

Falconara, Sicily. *Physics of the Earth and Planetary Interiors* 71: 100-111.

Langereis C. G., Zachariasse W. J. & Zijderveld J. D. A. 1984. — Late Miocene magnetostratigraphy of Crete. *Marine Micropaleontology* 8: 261-281.

McClelland E., Finegan B. & Butler R. W. H. 1996. — A magnetostratigraphic study of the onset of the Mediterranean Messinian salinity crisis; Caltanissetta Basin, Sicily, *in* Palaeomagnetism and Tectonics of the Mediterranean region, *Geological Society Special Publication* 105: 205-217.

McMillan K. J. 1979. — Radiolarian ratios and the Pleistocene-Holocene boundary. *Transactions. Gulf Coast Association of Geological Societies* 29: 298-301.

— 1981. — Radiolarians from the southern Mexico active margin: 643-652. *in* Watkins J. S., Moore J. C. *et al.* (eds), *Initial Reports of the Deep Sea Drilling Project.* U.S. Governmental Printing Office, Washington D.C.

Meulenkamp J. E., Driever B. W. M., Jonkers H. A., Spaak P., Zachariasse W. J. & van der Zwaan G. J. 1979. — Late Miocene-Pliocene climatic fluctuations and marine cyclic sedimentation patterns. *Annales Géologiques du Pays Hellenique* II : 831-842.

Mottura S. 1871. — Sulla formazione terziaria nella zona solfifera della Sicilia, *in Memorie per servire alla Carta Geologica d'Italia del Comitato Geologico.* Vol. I. Firenze.

Mullineaux L. S. & Westberg-Smith W. J. 1986. — Radiolarians as paleoceanographic indicators in the Miocene Monterey Formation, Upper Newport Bay, California. *Micropaleontology* 32 (1): 48-71.

Müller C. 1985. — Late Miocene to Recent Mediterranean biostratigraphy and paleoenvironments based on calcareous nannoplankton: 471-485, *in* Stanley D. J. & Wezel F. C. (eds), *Geological evolution of the Mediterranean Basin.* Springer-Verlag, New York, Berlin, Heidelberg and Tokyo.

Nigrini C. & Lombari G. 1984. — Guide to Miocene Radiolaria. *Special Publication Cushman Foundation for Foraminiferal Research* No. 22, 422 p.

Nigrini C. & Moore T. C. J. 1979. — Guide to Modern Radiolaria. *Special Publication Cushman Foundation for Foraminiferal Research* No. 16, 342 p.

Nicotra F. 1882. — Diatomeae in schistis quibusdam messanensibus detectae. *Bollettino Societa' Geologica Italiana* 1: 1-45.

Palmer A. A. 1986. — Cenozoic radiolarians as indicators of neritic versus oceanic conditions in continental-margin deposits: U.S. Mid-Atlantic Coastal Plain. *Palaios* 1: 122-132.

Pedley H. M. & Grasso M. 1993. — Controls on fauna and sediment cyclicity within the Tripoli and Calcare di Base basins (late Miocene) of central Sicily. *Palaeogeography Palaeoclimatology Palaeoecology* 105: 337-360.

Petrushevskaya M. G. 1971. — Radiolyarii Nassellaria v planktone mirovogo okeana *in* Bykhovshii B. E. (ed.), Radiolyarii Mirovogo Okeana po materialam Sovetskikh Ekspeditisii, *Issled. Fauny Morei*, Nauka, Leningrad 9: 3-294 [in Russian].

— 1981. — Radiolaria of the order Nassellaria of the World Ocean, *in* Naumov D. V. (ed.), *Description of the fauna of the USSR*, Zoological Institute, Academy of Science, USSR, 128: 1-406 [in Russian].

Riedel W. R. & Sanfilippo A. 1978. — Radiolaria, *in* Zachariasse W. J., Riedel W. R., Sanfilippo A., Schmidt R. R., Börsma M. J., Schrader H. J., Gersonde R., Drooger M. M. & Broekman J. A. (eds), Micropaleontological Counting Methods and Techniques. An Exercise on an Eight Metre Section of the Lower Pliocene of Capo Rossello, Sicily, *Utrecht Micropaleontological Bulletins* No. 17: 81-128.

Riedel W. R., Sanfilippo A. & Cita M. B. 1974. — Radiolarians from the stratotype Zanclean (Lower Pliocene, Sicily). *Rivista Italiana di Paleontologia e Stratigrafia* 80 (4): 699-734.

Riedel W. R., Westberg-Smith M. J. & Budai A. 1985. — Late Neogene Radiolaria and Mediterranean Paleoenvironments: 487-523, *in* Stanley D. J. & Wezel F.-C. (eds), *Geological Evolution of the Mediterranean Basin.* Springer Verlag, New York, Berlin, Heidelberg and Tokyo.

Rio D., Thunell R., Sprovieri R., Bukry D., Di Stefano E., Howell M., Raffi I., Sancetta C. & Sanfilippo A. 1989. — Stratigraphy and depositional history of the Pliocene Bianco section, Calabria, southern Italy. *Palaeogeography, Palaeoclimatology, Palaeoecology* 76 (1-2): 85-105.

Sanfilippo A. 1971. — Neogene radiolarians of the Mediterranean and western Pacific. *Proceedings of the II Planktonic Conference, Roma, 1970*: 1121-1127.

— 1974. — Pliocene radiolaria from Bianco, Calabria, Italy. *Micropaleontology* 34 (2): 159-180.

Sanfilippo A., Burkle L. H., Martini E. & Riedel W. R. 1973. — Radiolarians, Diatoms, Silicoflagellates and calcareous nannofossils in the Mediterranean Neogene. *Micropaleontology* 19 (2): 209-234.

Sauvage H. E. 1873. — Mémoire sur la faune ichthyologique de la période tertiaire et plus spécialement sur les poissons fossiles d'Oran (Algérie) et sur ceux découverts par M. R. Alby à Licata en Sicile. *Annales des Sciences Géologique*, Paris 4 (1) : 1-272.

Schwager C. 1878. — Nota su alcuni Foraminiferi nuovi del Tubo die stretto. *Bollettino Regio Comitato Geologico Italiano* IX: 519-531.

Sprovieri R., Di Stefano E. & Sprovieri M. 1996. — High resolution chronology for Late Miocene Mediterranean stratigraphic events. *Rivista Italiana di Paleontologia e Stratigrafia* 102 (1): 77-104.

Stöhr E. 1876. — Il terreno pliocenico dei dintorni di Girgenti. *Bollettino Regio Comitato Geologico*

Italiano VII (11-12).
— 1878. — Sulla posizione geologica del tufo e del tripoli nella zona solfifera di Sicilia. *Bollettino Regio Comitato Geologico Italiano* 11-12: 498-518.
Suc J. P., Violanti D., Londeix L., Poumot C., Robert C., Clauzon G., Gautier F., Turon J. L., Ferrier J., Chikhi H. & Cambon G. 1995. — Evolution of the Messinian Mediterranean environments: the Tripoli Formation at Capodarso (Sicily, Italy), *in* Verniers J., Poumot C. & Streel M. (eds), *Marine quantitative palynology: tectonic, climatic and eustatic control, [Review of Palaeobotany and Palynology]* 87(1): 51-79.
Swanberg N. R. & Bjørklund K. R. 1986. — The radiolarian fauna of western Norwegian fjords: Patterns of abundance in the plankton. *Marine Micropaleontology* 11: 231-241.
— 1987. — Radiolaria in the plankton of some fjord in western Norway: The distribution of species. *Sarsia* 72: 231-244.
Theodorites S. 1984. — Calcareous nannofossil biozonation of the Miocene and revision of the helicoliths and discoasters. *Utrecht Micropaleontological Bulletin* 32: 1-271.
Theyer F. & Hammond S. R. 1974. — Paleomagnetic polarity sequence and radiolarian zones, Brunhes to polarity Epoch 20. *Earth and Planetary Science Letters* 22: 307-319.
Vai G. B. 1997. — Cyclostratigraphic estimate of the Messinian stage duration, *in* Montanari A., Odin G. S. and Coccioni R. (eds), Miocene stratigraphy: An integrated approach, *Developements in Paleontology and Stratigraphy* 15: 463-476.
van der Zwaan G. J. 1982. — Paleontology of Late Miocene Mediterranean foraminifera. *Utrecht Micropaleontological Bulletin* 25: 1-201.
van der Zwaan G. J. & Gudjonsson L. 1986. — Middle Miocene-Pliocene stable isotope stratigraphy and paleoceanography of the Mediterranean. *Marine Micropaleontology* 10: 71-90.

Submitted for publication on 27 April 1998;
accepted on 11 June 1999.

APPENDIX

TABLE 1. — The taxa which have been identified and counted for the statistical exercise in this study. Literature references are given to illustrations of the most important taxa.

	Taxa	References for illustrations
1	*Botryopyle* sp.	Fig. 20A-E
2	*Acrobotrys* sp. cf. *A. disolenia*	Petrushevskaya (1981; fig. 495)
3	*Actinomma* sp. cf. *A. medianum*	Nigrini & Moore (1979; pl. 3, fig. 5)
4	*Actinomma* sp.	
5	*Actinomma* sp. 1	
6	*Amphirrhopalum* sp.	
7	*Anomalocantha dentata*	Nigrini & Moore (1979; pl. 4, fig. 4)
8	*Anthocyrtidium ehrenbergi*	Fig. 21F, J; Nigrini & Lombari (1984; pl. 27, figs 1-2)
9	*Arachnocorallium* sp.	Riedel *et al.* (1985; pl. 3, figs 13a-c)
10	*Hymeniastrum* sp.	Riedel *et al.* (1985; pl. 2, fig. 2a)
11	*Botryostrobus auritus/australis*	Fig. 21K, N; Riedel *et al.* (1985; pl. 5, fig. 7)
12	*Carpocanarium papillosum*	Nigrini & Moore (1979; pl. 21, fig. 3)
13	*Carpocanistrum* sp.	Fig. 21O, S; Riedel *et al.* (1985; pl. 5, figs 2-3)
14	*Cenosphaera cristata*?	Nigrini & Moore (1979; pl. 4, figs 2a-b)
15	*Cenosphaera* sp. 2	Fig. 20B, E; Nigrini & Moore (1979; pl. 4, fig. 3b)
16	*Ceratocyrtis* sp.	Riedel *et al.* (1985; pl. 3, fig. 14b)
17	*Cornutella profunda*	Fig. 21G, I; Nigrini & Lombari (1984; pl. 22, fig. 1)
18	*Cyrtocapsella cylindroides*	Nigrini & Lombari (1984; pl. 23, fig. 2)
19	*Didymocyrtis* sp.	Fig. 21G, J; Nigrini & Moore (1979; pl. 4, fig. 3b)
20	*Euchitonia furcata*	Nigrini & Lombari (1984; pl. 8, fig. 1)
21	*Eucyrtidium cienkowskii*	Nigrini & Lombari (1984; pl. 23, fig. 6)
22	*Eucyrtidium hexagonatum*	Nigrini & Lombari (1984; pl. 23, fig. 8)
23	*Eucyrtidium* sp. cf. *E. holospira*	Petrushevskaya (1981; fig. 295)
24	*Eucyrtidium punctatum*	Fig. 22R, W; Riedel *et al.* (1974, pl. 62, Fig. 6)
25	*Heliodiscus asteriscus*	Nigrini & Lombari (1984; pl. 5, Fig. 4)
26	*Heliodiscus echiniscus*	Riedel *et al.* (1974, pl. 56, Fig. 5)
27	*Hexacontium arachnoidale*	Fig. 20D; Hollande & Enjumet (1960, pl. LIII, Fig. 1)
28	*Hexacontium pachydermum* (big)	Fig. 20F; Riedel *et al.* (1985; pl. 1, Fig. 6a)
29	*Hexacontium pachydermum* (small)	Fig. 20C; Riedel *et al.* (1985; pl. 1, Fig. 6c)
30	*Hexacontium* sp.	
31	*Hexapyle* sp.	
32	*Hymeniastrum* sp.	Fig. 20I; Riedel *et al.* (1985; pl. 2, Fig. 2b)
33	*Larcoid* sp. 1 (spiral)	
34	*Larcoid* sp. 2 (small)	
35	Larcoidea sp.	Fig. 20K, L
36	*Larcopyle buetschlii*	Nigrini & Moore (1979; pl. 17, figs 1a-b)
37	*Larcopyle* sp.	Riedel *et al.* (1985; pl. 2, figs 11a-b)
38	*Larcospira quadrangula*	Nigrini & Lombari (1984; pl. 13, Fig. 3)
39	*Lipmanella* sp.	Riedel *et al.* (1985; pl. 4, Fig. 9)
40	*Litharachnium* sp.	Fig. 22M; Riedel *et al.* (1985; pl. 4, fig.11)
41	*Lithomelissa* sp. cf. *L. setosa*	Fig. 22F-L; Riedel *et al.* (1985; pl. 3, fig.15c)
42	*Lithomitra arachnea*	Riedel *et al.* (1985; pl. 5, Fig. 8b)
43	*Lithomitra* sp. cf. *L. lineata*	Fig. 21H, L, M; Riedel *et al.* (1985; pl. 5, Fig. 8a)
44	*Lophophaena buetschlii*	Petrushevskaya (1971, Fig. 58 I-X)
45	*Lophophaena* sp.	Fig. 21O, S
46	*Tetrapyle octacantha*	Nigrini & Lombari (1984; pl. 12, Fig. 3)
47	*Phormostichoartus corbula*	Nigrini & Lombari (1984; pl. 31, Fig. 4)
48	*Phorticium polycladum*	Nigrini & Lombari (1984; pl. 12, Fig. 1)
49	*Porodiscus* sp.	Riedel *et al.* (1985; pl. 2, figs 3-4)
50	*Pterocanium* sp.	Riedel *et al.* (1974, pl. 60, figs 4-6)
51	*Spongaster berminghami*	Nigrini & Lombari (1984; pl. 9, Fig. 1)
52	*Spongotrochus glacialis*	Nigrini & Lombari (1984; pl. 11, Fig. 2)

	Taxa	References for illustrations
53	*Spongotrochus resurgens osculosa*	Gig. 20A; Nigrini & Lombari (1984; pl. 11, Fig. 1)
54	*Hexalonche* sp.	
55	*Stichocorys delmontensis*	Fig. 21A-E; Nigrini & Lombari (1984; pl. 25, Fig. 4)
56	*Stichocorys delmontensis* (dwarf)	
57	*Stichocorys delmontensis* (thick)	
58	*Stichocorys delmontensis* (thin)	
59	*Stichocorys peregrina*?	Nigrini & Lombari (1984; pl. 25, Fig. 6)
60	*Stylochlamydium venustum*	Fig. 20M; Nigrini & Lombari (1984; pl. 11, Fig. 3)
61	*Stylodictya aculeata*	Jørgensen (1905, pl X, Fig. 41)
62	*Stylodictya tenuispina*	Bjørklund (1976, pl. 4, Fig. 5)
63	*Stylodictya validispina*	Bjørklund (1976, pl. 4, fig. 4)
64	*Stylosphaera angelina*	Riedel *et al.* (1974, pl. 56, fig. 2)
65	*Thecosphaera grecoi*	Fig. 20H; Riedel *et al.* (1974, pl. 56, fig. 3)
66	*Theocapsa? cretica*	Fig. 22T-V Riedel *et al.* (1985; pl. 4, fig. 15)
67	Trissocyclidae sp.	Fig. 21T-Y
68	*Zygocircus productus*	Nigrini & Lombari (1984; pl. 15, figs 1-2)

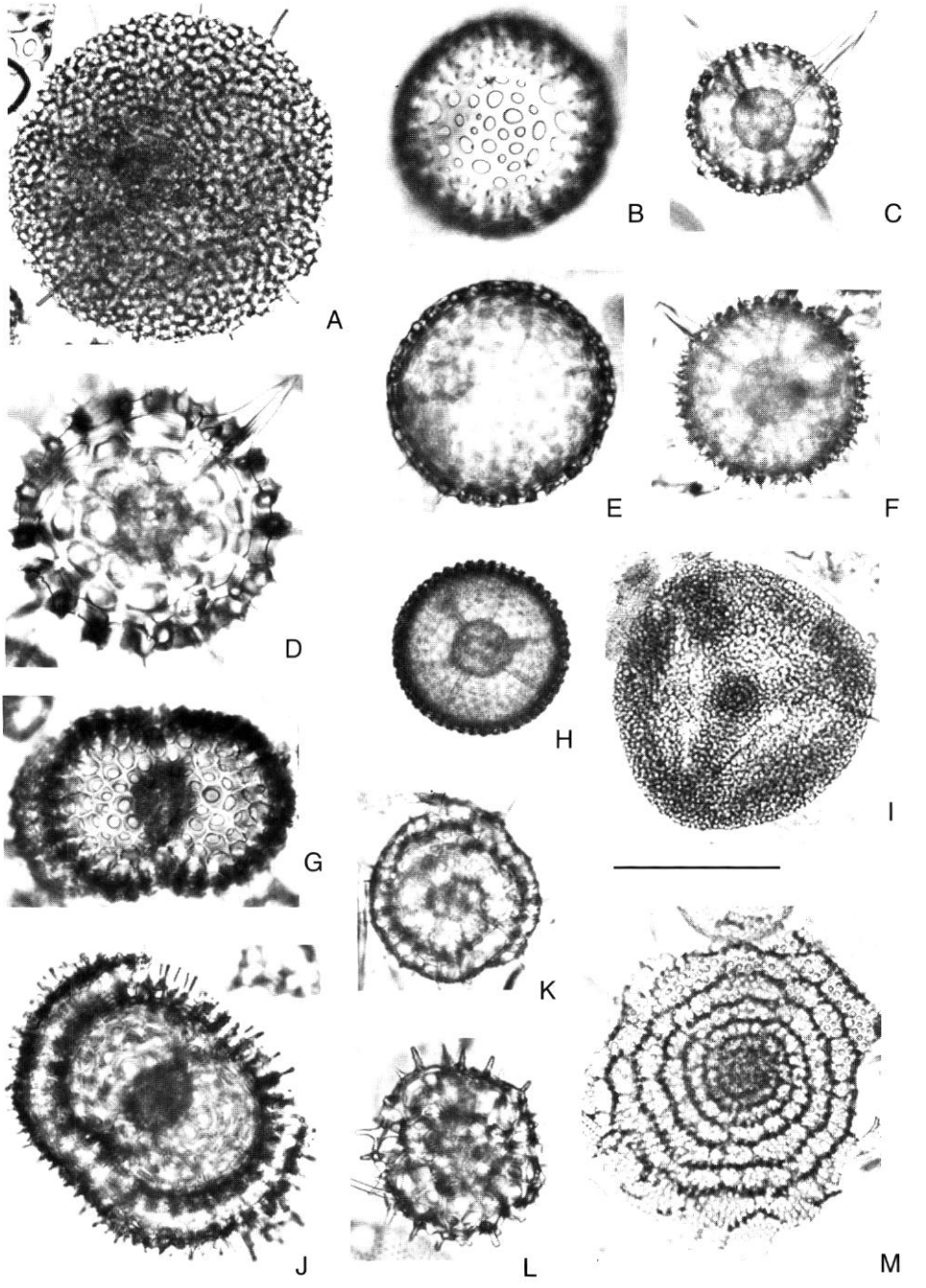

FIG. 20. — **A**, *Spongotrochus glacialis/osculosa* (D26.11); **B**, **E**, *Cenosphaera* sp. 2 (D20.2); **C**, *Hexacontium pachydermum* (small) (D20.2); **D**, *Hexacontium arachnoidale* (D20.2); **F**, *Hexacontium pachydermum* (big) (D31.2); **G**, **J**, *Didymocyrtis* sp. (D26.11); **H**, *Thecosphaera grecoi* (D27.2); **I**, *Hymeniastrum* sp. **K**, **L**, Larcoidea sp. (D27.2); **M**, *Stylochlamydium venustum* (D27.2). Scale bar: 100 µm.

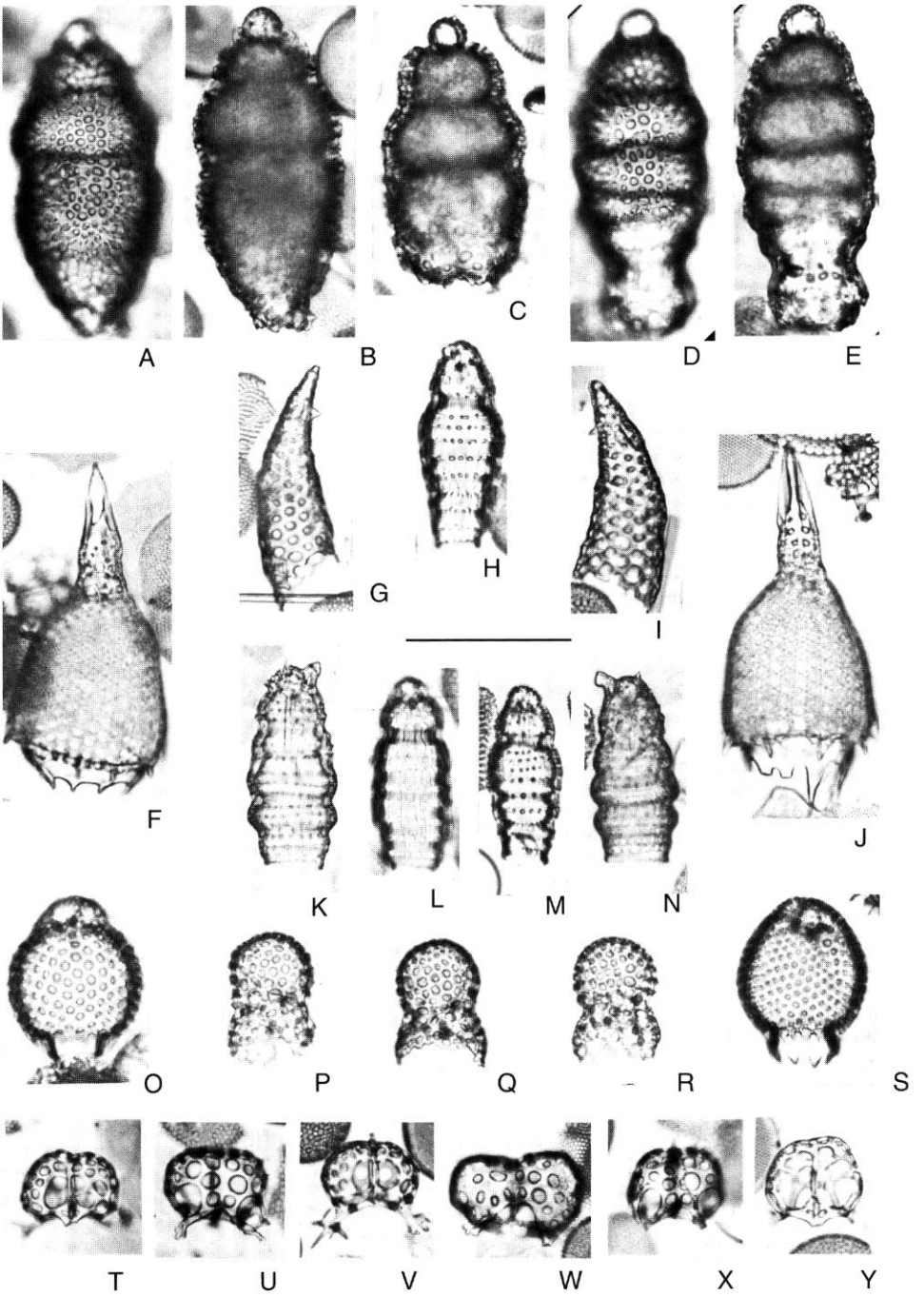

FIG. 21. — **A-E**, *Stichocorys delmontensis* (D17.1); **F**, **J**, *Anthocyrtidium ehrenbergi* (D20.2); **G**, **I**, *Cornutella profunda* (D17.1); **H**, **L**, **M**, *Lithomitra lineata* (D4.9); **K**, **N**, *Botryostrobus auritus/australis* (D21.22); **O**, **S**, *Carpocanistrum* sp. (D26.11); **P-R**, *Lophophaena* sp. (D26.11); **T-Y**, Trissocyclidae sp. (D17.1). Scale bar: 100 µm.

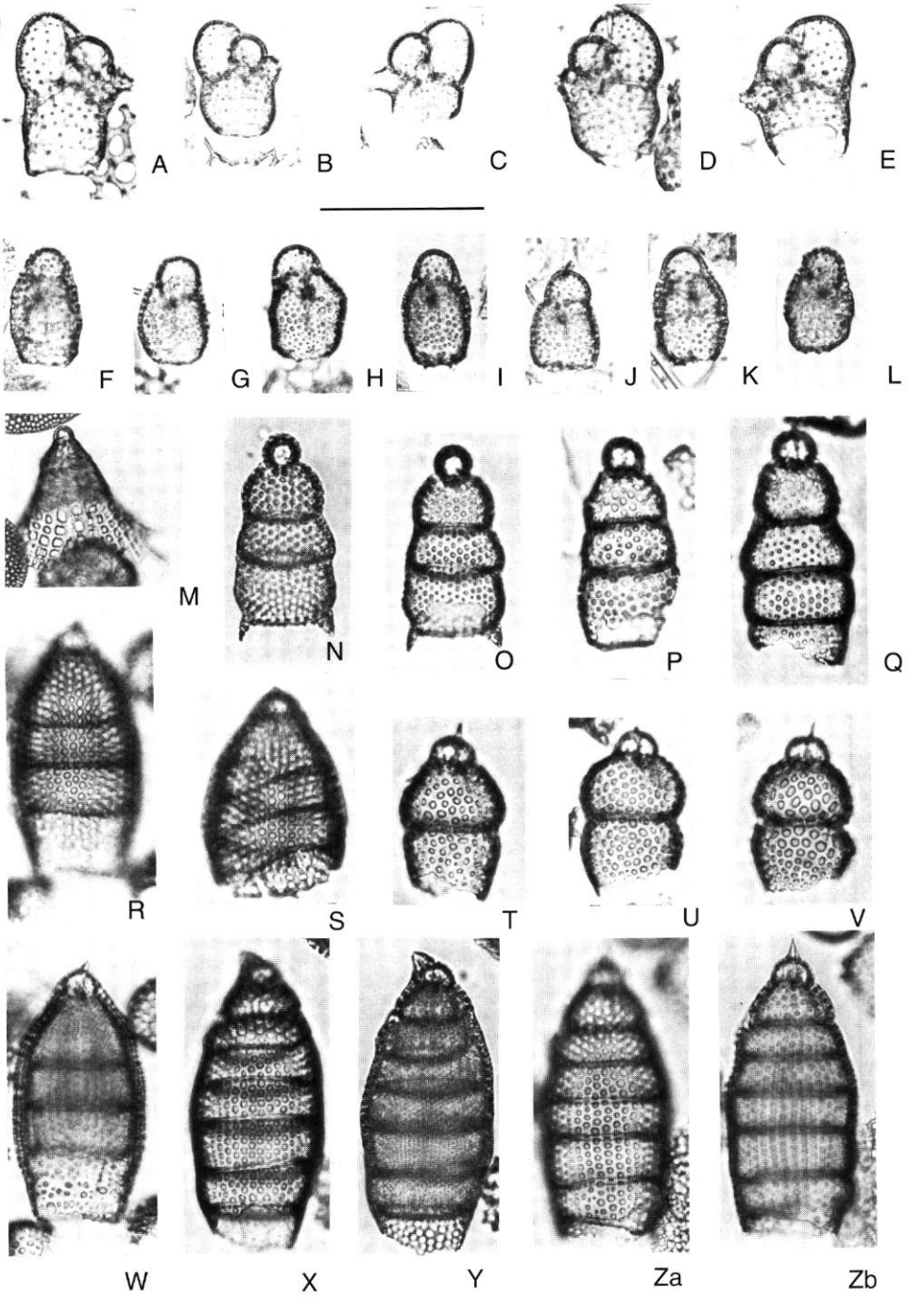

FIG. 22. — **A-E**, *Botryopyle* sp. (D26.11); **F-L**, *Lithomelissa* sp. cf. *L. setosa* (D28.0); **M**, *Litharachnium* sp. (D26.11); **N-Q**, *Stichocorys delmontensis* (D26.11); **R**, **W**, *Eucyrtidium punctatum* (D26.11), same specimen; **S**, *Eucyrtidium* sp. cf. *E. holospira* (D26.11); **T-V**, *Theocapsa* ? *cretica*; **X-Zb**, *Eucyrtidium* sp. (D26.11). Scale bar: 100 µm.

TABLE 2. — Estimated age above section base, radiolarian flux, number of radiolarians per gram $CaCO_3$-free sediment, number of nassellarians, spumellarians and radiolarians per gram bulk sediment, Spumellaria/Nassellaria ratio, $CaCO_3$ and TOC content for each of the samples collected during the 1995 field-trip (one sample for each lithology).

Sample Code	Years above Section base	Flux in ky/cm²	Rads gcf	Number of Spum/g	Number of Nass/g	Number of Rads/g	S/N ratio	Percent $CaCO_3$	Percent TOC
D 36	757000	23698	82123	28553	12437	40990	2.30	50.09	0.100
D 35	736000	1351	1447	173	1038	1211	0.17	16.29	0.095
D 34	715000	8397	6595	810	5263	6073	0.15	7.92	0.000
D 33	694000	108560	269415	107042	33627	140669	3.18	47.79	0.116
D 32	673000	27978	37831	14613	5874	20487	2.49	45.85	0.139
D 31	652000	48261	55561	23518	20356	43874	1.16	21.04	0.096
D 30	631000	3261	4787	1786	2273	4058	0.79	15.22	0.144
D 29	610000	8967	8240	2141	4587	6728	0.47	18.35	0.158
D 28	589000	61163	73836	19427	14417	33845	1.35	54.16	0.131
D 27	567000	24777	41790	7242	5850	13092	1.24	68.67	0.070
D 26	546000	303644	258157	95126	74368	169495	1.28	34.34	0.129
D 21	525000	57511	71345	14480	20916	35396	0.69	50.39	0.174
S 21	504000	3217	2121	437	1310	1747	0.33	17.64	0.133
D 20	399000	46565	45089	12654	10328	22982	1.23	49.03	0.117
S 20	399000	139	155	98	0	98	>1	36.62	0.106
D 19	378000	101764	65397	16756	28966	45722	0.58	30.09	0.120
S 19	378000	0	0	0	0	0	–	17.76	0.069
D 18	357000	31793	64398	20134	32215	52349	0.63	18.71	0.115
S 18	357000	15897	34789	9099	12408	21507	0.73	38.18	0.139
D 17	336000	63761	54258	14449	29106	43555	0.50	19.73	0.113
S 17	336000	0	0	0	0	0	–	33.52	0.118
D 16	315000	40402	118495	20516	39013	59529	0.53	49.76	0.129
S 16	315000	0	0	0	0	0	–	23.73	0.063
D 15	294000	110185	109436	22199	46934	69133	0.47	36.83	0.091
S 15	294000	505	500	312	0	312	>1	37.68	0.139
S 14	273000	0	0	0	0	0	–	40.49	0.121
D 13	273000	62848	76710	21456	24369	45825	0.88	40.26	0.149
S 13	252000	1598	2033	1463	0	1463	–	28.02	0.148
D 12	231000	39217	48788	17328	13017	30345	1.33	37.80	0.144
S 12	231000	0	0	0	0	0	–	24.38	0.115
D 11	210000	54022	43391	7658	24324	31982	0.31	26.29	0.165
S 11	210000	77799	55215	26947	16105	43053	1.67	22.03	0.167
D 10	189000	41511	35230	14907	12836	27743	1.16	21.25	0.150
S 10	189000	0	0	0	0	0	–	16.07	0.112
D 9	168000	117065	53363	21005	19977	40982	1.05	23.20	0.166
S 9	168000	0	0	0	0	0	–	25.59	0.110
D 8	147000	52728	33096	15088	12665	27753	1.19	16.14	0.173
S 8	147000	0	0	0	0	0	–	13.67	0.150
D 7	126000	124783	50841	15618	27358	42977	0.57	15.47	0.144
S 7	126000	609	284	115	115	230	1.00	18.82	0.172
D 6	105000	109467	44065	18243	17761	36004	1.03	18.29	0.105
S 6	105000	293	173	0	122	122	<1	29.35	0.178
D 5	84000	89435	66214	17864	18447	36311	0.97	45.16	0.111
S 5	84000	478	306	117	117	234	1.00	23.64	0.154
D 4	63000	45446	34871	13299	10000	23299	1.33	33.19	0.118
S 4	63000	0	0	0	0	0	–	30.59	0.070
D 3	42000	0	0	0	0	0	–	34.48	0.083
D 2	21000	0	0	0	0	0	–	28.94	0.058
S 2	21000	190	169	0	120	120	<1	29.20	0.166

TABLE 3. — Number of nassellarians, spumellarians and radiolarians per gram bulk sediment and S/N ratio for each of the samples of diatomite D7. Cycle 7 is 84.9 cm thick, with the diatomite and claystone lithologies making up 46.9 and 38 cm, respectively.

Sample Number	Distance from base (cm)	(%)	Years from base cycle	section	Number of Spum/g	Nass/g	Rads/g	Spum/Nass ratio
F97- Dia 7.28	84.9	1.000	21000	147000	13686	21773	35459	0.63
F97- Dia 7.27	82.6	0.973	20431	146431	12306	21632	33938	0.57
F97- Dia 7.26	81.2	0.956	20085	146085	11261	15878	27140	0.71
F97- Dia 7.25	79.7	0.939	19714	145714	13445	20483	33929	0.66
F97- Dia 7.24	78.2	0.921	19343	145343	17670	24537	42207	0.72
F97- Dia 7.23	76.0	0.895	18799	144799	19434	29434	48868	0.66
F97- Dia 7.22	75.1	0.885	18576	144576	14175	18986	33162	0.75
F97- Dia 7.21	73.0	0.860	18057	144057	14725	29126	43851	0.51
F97- Dia 7.20	72.1	0.849	17834	143834	15123	30435	45558	0.50
F97- Dia 7.19	70.3	0.828	17389	143389	15570	26023	41594	0.60
F97- Dia 7.18	68.0	0.801	16820	142820	18945	34892	53837	0.54
F97- Dia 7.17	66.5	0.783	16449	142449	17131	27888	45020	0.61
F97- Dia 7.16	64.8	0.763	16028	142028	27557	33239	60795	0.83
F97- Dia 7.15	63.1	0.743	15608	141608	25047	36622	61670	0.68
F97- Dia 7.14	61.4	0.723	15187	141187	16997	23597	40594	0.72
F97- Dia 7.13	60.4	0.711	14940	140940	24356	33262	57618	0.73
F97- Dia 7.12	59.0	0.695	14594	140594	29529	37059	66588	0.80
F97- Dia 7.11	57.5	0.677	14223	140223	29266	41253	70518	0.71
F97- Dia 7.10	56.0	0.660	13852	139852	21444	34914	56358	0.61
F97- Dia 7.9	54.4	0.641	13456	139456	14881	25794	40675	0.58
F97- Dia 7.8	52.7	0.621	13035	139035	18472	35694	54167	0.52
F97- Dia 7.7	50.2	0.591	12417	138417	17090	39594	56684	0.43
F97- Dia 7.6	48.3	0.569	11947	137947	25338	52196	77534	0.49
F97- Dia 7.5	46.5	0.548	11502	137502	30425	33884	64308	0.90
F97- Dia 7.4	44.8	0.528	11081	137081	28993	24029	53022	1.21
F97- Dia 7.3	43.0	0.506	10636	136636	72072	45195	117267	1.59
F97- Dia 7.2	41.3	0.486	10216	136216	38832	60745	99577	0.64
F97- Dia 7.1	39.6	0.466	9795	135795	49799	36419	86217	1.37

TABLE 4. — Number of nassellarians, spumellarians and radiolarians per gram bulk sediment and S/N ratio for each of the samples of diatomite D21. Cycle 21 is 74 cm thick, with the diatomite and claystone lithologies making up 64 and 10 cm, respectively.

Sample Number	Distance from base (cm)	(%)	Years from base cycle	section	Number of Spum/g	Nass/g	Rads/g	Spum/Nass ratio
F95- Dia 21.0	74.0	1.000	21000	420000	16311	26866	43177	0.61
F95- Dia 21.1	73.0	0.986	20716	419716	15772	24497	40268	0.64
F95- Dia 21.2	72.0	0.973	20432	419432	15846	24311	40157	0.65
F95- Dia 21.3	71.0	0.959	20149	419149	21343	27655	48998	0.77
F95- Dia 21.4	70.0	0.946	19865	418865	22346	17318	39665	1.29
F95- Dia 21.5	69.0	0.932	19581	418581	15962	21009	36972	0.76
F95- Dia 21.6	68.0	0.919	19297	418297	13426	23495	36921	0.57
F95- Dia 21.7	67.0	0.905	19014	418014	16762	19810	36571	0.85
F95- Dia 21.8	66.0	0.892	18730	417730	11816	24378	36194	0.48
F95- Dia 21.9	65.0	0.878	18446	417446	18607	16895	35502	1.10
F95- Dia 21.10	64.0	0.865	18162	417162	15256	22692	37949	0.67
F95- Dia 21.11	63.0	0.851	17878	416878	16951	19723	36674	0.86
F95- Dia 21.12	62.0	0.838	17595	416595	10808	17795	28603	0.61
F95- Dia 21.13	61.0	0.824	17311	416311	17584	21292	38876	0.83
F95- Dia 21.14	59.5	0.804	16885	415885	10758	23182	33939	0.46
F95- Dia 21.15	58.0	0.784	16459	415459	11364	23529	34893	0.48
F95- Dia 21.16	56.5	0.764	16034	415034	16412	23282	39695	0.70
F95- Dia 21.17	55.0	0.743	15608	414608	11944	25833	37778	0.46
F95- Dia 21.18	53.5	0.723	15182	414182	10976	23018	33994	0.48
F95- Dia 21.19	52.0	0.703	14757	413757	8411	19938	28349	0.42
F95- Dia 21.20	50.5	0.682	14331	413331	12791	33866	46657	0.38
F95- Dia 21.21	49.0	0.662	13905	412905	12431	27901	40331	0.45
F95- Dia 21.22	47.5	0.642	13480	412480	14480	20916	35396	0.69
F95- Dia 21.23	46.0	0.622	13054	412054	10853	21318	32171	0.51
F95- Dia 21.24	44.5	0.601	12628	411628	11887	22304	34191	0.53
F95- Dia 21.25	43.0	0.581	12203	411203	15833	27024	42857	0.59
F95- Dia 21.26	41.5	0.561	11777	410777	13523	13295	26818	1.02
F95- Dia 21.27	40.0	0.541	11351	410351	12529	14988	27518	0.84
F95- Dia 21.28	38.5	0.520	10926	409926	10684	13355	24038	0.80
F95- Dia 21.29	37.0	0.500	10500	409500	10462	14402	24864	0.73
F95- Dia 21.30	35.5	0.480	10074	409074	14321	18272	32593	0.78
F95- Dia 21.31	34.0	0.459	9649	408649	13921	16241	30162	0.86
F95- Dia 21.32	32.5	0.439	9223	408223	13079	16898	29977	0.77
F95- Dia 21.33	31.0	0.419	8797	407797	13270	14692	27962	0.90
F95- Dia 21.34	29.5	0.399	8372	407372	16085	22569	38653	0.71
F95- Dia 21.35	28.0	0.378	7946	406946	15179	13616	28795	1.11
F95- Dia 21.36	26.5	0.358	7520	406520	19036	21687	40723	0.88
F95- Dia 21.37	25.0	0.338	7095	406095	15556	14198	29753	1.10
F95- Dia 21.38	23.5	0.318	6669	405669	18750	17428	36178	1.08
F95- Dia 21.39	22.0	0.297	6243	405243	18810	19881	38690	0.95
F95- Dia 21.40	20.5	0.277	5818	404818	35455	21932	57386	1.62
F95- Dia 21.41	19.0	0.257	5392	404392	30383	26077	56459	1.17
F95- Dia 21.42	17.5	0.236	4966	403966	34852	23517	58369	1.48
F95- Dia 21.43	16.0	0.216	4541	403541	34709	14071	48780	2.47
F95- Dia 21.44	14.5	0.196	4115	403115	46758	29371	76130	1.59
F95- Dia 21.45	13.0	0.176	3689	402689	44615	41868	86484	1.07
F95- Dia 21.46	11.5	0.155	3264	402264	48364	42545	90909	1.14
F95- Dia 21.47	10.0	0.135	2838	401838	41189	72687	113877	0.57

TABLE 5. — Number of nassellarians, spumellarians and radiolarians per gram bulk sediment and S/N ratio for each of the samples of diatomite D28. Cycle 28 is 95.7 cm thick, with the diatomite and claystone lithologies making up 49.7 and 46 cm, respectively.

Sample Number	Distance from base (cm)	(%)	Years from base cycle	section	Number of Spum/g	Nass/g	Rads/g	Spum/Nass ratio
F97- Dia 28.36	95.7	1.000	21000	588000	6911	256	7167	27.00
F97- Dia 28.35	94.2	0.984	20671	587671	5876	100	5976	59.00
F97- Dia 28.34	92.5	0.967	20298	587298	5753	105	5858	55.00
F97- Dia 28.33	91.1	0.952	19991	586991	3035	160	3195	19.00
F97- Dia 28.32	89.9	0.939	19727	586727	4006	148	4154	27.00
F97- Dia 28.31	88.8	0.928	19486	586486	3482	418	3900	8.33
F97- Dia 28.30	87.6	0.915	19223	586223	5307	83	5390	64.00
F97- Dia 28.29	85.5	0.893	18762	585762	3765	235	4000	16.00
F97- Dia 28.28	84.0	0.878	18433	585433	3282	290	3571	11.33
F97- Dia 28.27	82.3	0.860	18060	585060	4340	362	4702	12.00
F97- Dia 28.26	80.6	0.842	17687	584687	3623	580	4203	6.25
F97- Dia 28.25	79.4	0.830	17423	584423	4364	285	4649	15.33
F97- Dia 28.24	77.7	0.812	17050	584050	3583	489	4072	7.33
F97- Dia 28.23	76.7	0.801	16831	583831	2490	1452	3942	1.71
F97- Dia 28.22	75.7	0.791	16611	583611	5724	818	6542	7.00
F97- Dia 28.21	74.3	0.776	16304	583304	5889	1501	7390	3.92
F97- Dia 28.20	73.0	0.763	16019	583019	8918	2778	11696	3.21
F97- Dia 28.19B	72.0	0.752	15799	582799	3101	1163	4264	2.67
F97- Dia 28.19A	70.8	0.740	15536	582536	6393	2295	8689	2.79
F97- Dia 28.18	69.8	0.729	15317	582317	5938	3438	9375	1.73
F97- Dia 28.17	68.7	0.718	15075	582075	7943	3010	10953	2.64
F97- Dia 28.16	67.4	0.704	14790	581790	7177	3589	10766	2.00
F97- Dia 28.15	66.3	0.693	14549	581549	6377	3050	9427	2.09
F97- Dia 28.14	64.9	0.678	14241	581241	8701	3016	11717	2.88
F97- Dia 28.13	63.7	0.666	13978	580978	12808	4803	17611	2.67
F97- Dia 28.12	62.5	0.653	13715	580715	19118	5042	24160	3.79
F97- Dia 28.11	61.5	0.643	13495	580495	21261	6944	28205	3.06
F97- Dia 28.10	60.4	0.631	13254	580254	18448	4580	23028	4.03
F97- Dia 28.9	58.5	0.611	12837	579837	17108	11153	28261	1.53
F97- Dia 28.8	57.2	0.598	12552	579552	18689	8611	27299	2.17
F97- Dia 28.7	55.9	0.584	12266	579266	33293	15865	49159	2.10
F97- Dia 28.6	54.7	0.572	12003	579003	36830	18192	55022	2.02
F97- Dia 28.5	53.3	0.557	11696	578696	27660	13032	40691	2.12
F97- Dia 28.4	52.2	0.545	11455	578455	41333	10917	52250	3.79
F97- Dia 28.3	50.5	0.528	11082	578082	42285	12725	55010	3.32
F97- Dia 28.2	49.1	0.513	10774	577774	35327	8323	43650	4.24
F97- Dia 28.1	47.1	0.492	10335	577335	41444	10444	51889	3.97

TABLE 6. — Varimax Factor Components Matrix (Samples *vs* Factors).

Samples	Factor 1	Factor 2	Factor 3	Factor 4	Factor 5	Factor 6	Factor 7	Factor 8	Factor 9
D36	0.082	0.724	0.078	-0.016	0.418	0.398	0.049	0.059	0.074
D35	0.007	0.149	0.009	-0.011	-0.003	0.904	-0.003	-0.011	-0.004
D34	0.858	0.175	0.092	-0.011	-0.079	-0.034	-0.001	0.425	-0.036
D33	0.043	0.423	0.048	-0.013	0.883	-0.021	0.092	-0.035	-0.003
D32	0.089	0.842	0.092	-0.029	0.489	0.044	0.091	0.042	0.093
D31	0.505	0.785	0.134	-0.025	0.223	0.048	0.021	-0.155	0.157
D30	0.111	0.894	0.108	0.247	-0.140	0.109	0.001	0.131	0.033
D29	0.115	0.863	0.043	-0.052	-0.113	-0.113	0.005	0.403	-0.010
D28	0.207	0.672	0.032	-0.062	0.024	-0.229	0.026	-0.281	-0.233
D27	0.122	0.901	0.124	0.003	-0.086	0.247	0.043	-0.094	0.031
D26	0.158	0.793	0.063	0.274	0.271	0.050	0.053	0.427	-0.011
D21	0.623	0.255	0.066	-0.011	-0.043	0.018	0.083	-0.003	0.708
S21	0.008	0.074	0.010	-0.001	0.086	0.005	0.993	0.003	0.034
D20	0.133	0.832	0.121	-0.026	0.263	0.052	0.048	-0.419	0.035
D19	0.976	0.141	0.120	-0.007	-0.013	0.000	0.010	-0.084	-0.073
D18	0.981	0.036	0.124	0.005	-0.036	0.045	0.009	-0.072	-0.003
S18	0.964	0.099	0.133	0.004	0.024	0.043	0.046	-0.109	-0.016
D17	0.958	0.197	0.138	-0.007	0.040	-0.001	0.027	-0.115	-0.035
D16	0.226	0.097	0.965	0.005	0.049	0.012	0.003	-0.070	0.009
S16	0.039	0.045	0.004	0.997	0.004	-0.017	0.000	0.000	-0.005
D15	0.695	-0.105	0.698	0.005	0.068	0.000	0.006	0.083	0.022
D13	0.978	0.059	0.108	0.011	0.118	0.037	0.016	0.070	0.079
S13	0.002	0.050	-0.005	0.997	0.004	-0.013	0.007	0.009	-0.006
D12	0.022	0.508	0.807	-0.005	-0.146	0.001	0.002	-0.087	0.139
D11	0.633	-0.109	0.755	0.004	0.024	-0.011	0.005	0.079	-0.026
S11	0.960	0.030	0.101	0.074	0.182	0.072	0.013	0.098	-0.002
D10	-0.069	0.115	0.982	0.000	0.109	-0.011	0.001	-0.021	0.018
D9	0.870	0.259	0.110	-0.010	0.010	0.013	0.011	-0.045	0.398
D8	0.121	0.800	0.065	-0.041	0.171	-0.112	0.019	-0.008	0.499
D7	0.984	0.112	0.122	-0.005	0.053	0.008	0.014	0.012	0.014
D6	0.934	0.226	0.116	-0.012	-0.043	-0.023	0.011	-0.115	0.200
D5	0.448	0.113	0.876	0.001	0.052	0.021	0.017	0.116	0.038
D4	0.876	0.206	0.321	-0.004	0.111	0.082	0.042	0.176	0.079
Var.	35,414	22,699	14,255	6,486	4,792	3,507	3,110	2,951	3,304
Cum. Var.	35,414	58,113	72,368	78,854	83,646	87,153	90,263	93,215	96,519

TABLE 7. — Scaled Varimax Factor Scores Matrix (Species *vs* Factor Scores). Absolute values of factor scores higher than one have been outlined.

	Factor 1	Factor 2	Factor 3	Factor 4	Factor 5	Factor 6	Factor 7	Factor 8	Factor 9
Anthocyrtidium ehrenbergi	-0.037	-0.048	0.000	0.011	-0.262	-0.014	3.111	0.018	0.065
Botryostrobus auritus/australis	0.183	0.264	-0.088	-0.058	-0.209	-0.488	-0.030	-0.300	3.360
Carpocanistrum sp.	0.000	0.060	0.005	-0.002	0.309	0.012	1.819	0.036	-0.073
Cenosphaera sp. 2	-0.005	-0.024	-0.012	-0.016	-0.164	1.939	-0.014	-0.197	-0.016
Didymocyrtis sp.	0.006	0.147	-0.031	3.595	0.013	-0.065	-0.010	0.020	-0.026
Larcoidea sp.	0.169	2.160	0.198	0.002	-0.220	1.116	0.046	0.705	0.465
Lithomelissa sp. cf. *L. setosa*	0.266	1.239	-0.136	-0.224	-0.599	-1.082	0.003	-0.767	-1.197
Lithomitra sp. cf. *L. lineata*	-0.376	-0.307	3.547	0.022	-0.010	-0.093	-0.009	0.176	0.034
Porodiscus sp.	0.068	1.282	0.151	-0.077	3.249	-0.164	0.059	-0.349	-0.027
Spongotrochus glacialis/osculosa	0.085	1.472	0.051	-0.102	-0.724	-0.602	-0.068	2.540	-0.168
Stichocorys delmontensis	3.535	-0.509	0.316	0.018	0.161	0.099	0.032	0.298	-0.087
Theocapsa ? cretica	-0.050	0.095	-0.014	-0.033	-0.046	2.484	-0.021	0.029	-0.095
Trissocyclidae sp.	0.459	1.591	0.473	0.018	-1.118	-0.002	-0.009	-2.256	-0.089

TABLE 8. — Factor component peaks (values higher than 0.400) used to establish the most important "radiolarian factor peaks" throughout the section. The peaks are coded as X.Y, where X represents the factor number and Y represents a reference number for the "factor peaks", arranged in an ascending order from base to top of the section.

Samples	Factor Peaks	Factor Component	Sapropel Age (Ma)	Diatomite Age (Ma)	Astro. ages	Tripoli Cycles
D36	2.12	0.724		6.183		
S36			6.194		6.132	T43
D35	6.1	0.904		6.204		
S35			6.215		6.145	T42
D34	1.16	0.858		6.225		
	8.4	0.425				
S34			6.236		6.164	T41
D33	2.11	0.423		6.246		
	5.2	0.883				
S33			6.257		6.184	T40
D32	2.10	0.842		6.267		
	5.1	0.489				
S32			6.278		6.205	T39
D31	1.15	0.505		6.288		
	2.9	0.785				
S31			6.299		6.226	T38
D30	2.8	0.894		6.309		
S30			6.320		6.257	T37
D29	2.7	0.863		6.331		
	8.3	0.403				
S29			6.342		6.278	T36
D28	2.6	0.672		6.352		
S28			6.363		6.299	T35
D27	2.5	0.901		6.373		
S27			6.384		6.320	T34
D26	2.4	0.793		6.394		
	8.2	0.427				
S26			6.405		6.342	T33
D26						
S25					*	T32
D24						
S24					6.373	T31
D23						
S23					6.393	T30
D22						
S22					6.413	T29
D21	1.14	0.623		6.499		
	9.2	0.708				
S21	7.1	0.993	6.510		6.432	T28
D20	2.3	0.832		6.520		
	8.1	-0.419				
S20			6.531		6.452	T27
D19	1.13	0.976		6.541		
S19			6.552		6.470	T26
D18	1.12	0.981		6.562		
S18	1.11	0.964	6.572		6.490	T25
D17	1.10	0.958		6.583		
S17			6.594		6.509	T24
D16	3.6	0.965		6.604		
S16	4.2	0.997	6.614		6.524	T23

Samples	Factor Peaks	Factor Component	Sapropel Age (Ma)	Diatomite Age (Ma)	Astro. ages	Tripoli Cycles
D15	1.9	0.695		6.625		
	3.5	0.698				
S15			6.636		6.544	T22
D14						
S14					6.563	T21
D13	1.8	0.978		6.667		
S13	4.1	0.997	6.678		6.585	T20
D12	2.2	0.508		6.688		
	3.4	0.807				
S12			6.699		6.606	T19
D11	1.7	0.633		6.709		
	3.3	0.755				
S11	1.6	0.960	6.719		6.635	T18
D10	3.2	0.982		6.730		
S10			6.741		6.657	T17
D9	1.5	0.870		6.751		
S9			6.762		6.678	T16
D8	2.1	0.800		6.772		
	9.1	0.499				
S8			6.783		6.699	T15
D7	1.4	0.984		6.793		
S7			6.804		6.721	T14
D6	1.3	0.934		6.814		
S6			6.825		6.752	T13
D5	1.2	0.448		6.835		
	3.1	0.876				
S5			6.846		6.771	T12
D4	1.1	0.876		6.856		
S4			6.867		6.792	T11
D3				6.877		
S3			6.888		6.810	T10
D2				6.898		
S2			6.909		6.829	T9
D1				6.919		
S1			6.930		6.847	T8